SANDIA NATIONAL LABORATORIES
WASTE ISOLATION PILOT PLANT

ANALYSIS REPORT FOR CULEBRA FLOW AND TRANSPORT IN THE 2026 COMPLIANCE RECERTIFICATION APPLICATION PERFORMANCE ASSESSMENT
REVISION 0

JUSTIN WILGUS (Affiliate) Digitally signed by JUSTIN WILGUS (Affiliate) Date: 2025.11.13 17:46:32 -07'00'

Authentication

Author:	Justin Wilgus	Org.	8881
Author:	James Bethune	Org.	8881
Technical Reviewer:	Mahawa-Essa Mabossani Akara	Org.	8882
QA Reviewer:	Shelly R. Nielsen	Org.	8883
Management Reviewer:	Steve Wagner	Org.	8881

November 2025

Information Only

Executive Summary

The Waste Isolation Pilot Plant (WIPP) was initially certified as a repository consisting of 10 panels, which were excavated for the long-term storage and placement of transuranic waste (U.S. EPA 1998). However, due to operational constraints, the entire volume of the 10 panels is no longer available for waste disposal. In March 2024, the U.S. Department of Energy (DOE) submitted the Replacement Panels Planned Change Request (RPPCR) to the U.S. Environmental Protection Agency (EPA) for approval of waste emplacement in two new panels. These panels, referred to as replacement panels, are located to the west of the existing operations area. The EPA approved the RPPCR in July 2025 (U.S. EPA 2025).

The addition of the two replacement panels is not expected to provide adequate space for the disposal of the allowable waste volume designated for WIPP under the Land Withdrawal Act (LWA); thus, the 12-panel configuration is regarded as an interim state of the repository. The DOE may pursue approval for waste disposal in seven additional panels to accommodate the full allowable volume of waste. This hypothetical 19-panel configuration is considered the anticipated final state of the repository.

The DOE demonstrates compliance with containment requirements as outlined in the Certification Criteria of Title 40 CFR Part 191.13 through performance assessment (PA). PA calculations estimate the probability and consequences of potential radionuclide releases from the repository to the accessible environment over a regulatory period of 10,000 years following facility closure. WIPP PA models are utilized to support the periodic recertification of WIPP.

The 2026 Compliance Recertification Application (CRA-2026) represents the fifth recertification application submitted to the EPA. A PA has been carried out by Sandia National Laboratories to support the DOE's submission of the CRA-2026. The results presented in the CRA-2026 PA are compared to those from the RPPCR PA, the most recent regulatory submission.

The RPPCR considered the anticipated final state of the repository, which includes a total of 19 waste panels and represented releases to the Culebra with four distinct release points. The CRA-2026 12-panel configuration incorporates two of these mass release points while the 19-panel configuration employs four. This report analyzes transport from all four mass release points, encompassing Culebra flow and radionuclide transport components of the CRA-2026 PA for both the interim and final state repositories.

This report details the effects of the changes introduced and incorporated in the CRA-2026 PA that impact the Culebra flow and radionuclide transport model. In comparison to the RPPCR PA, the effects of these changes are isolated to Culebra release point 2, and primarily show slightly shorter travel times to the LWB and slight increases in radionuclide mass breakthrough.

Information Only

TABLE OF CONTENTS

EXECUTIVE SUMMARY II

1.0 INTRODUCTION 1

2.0 CHANGES SINCE THE RPPCR 2

2.1 Culebra Release Point Location 2

2.2 Parameters Not Updated as Anticipated in Analysis Plan AP-214 2

3.0 CONCEPTUAL APPROACH 3

3.1 Domain and Discretization 4

3.2 Boundary and Initial Conditions 8

3.3 Uncertainty 9

3.3.1 Subjective Uncertainty 9

3.3.2 Stochastic Uncertainty 9

4.0 CULEBRA MODEL METHODOLOGY 11

4.1 Mining Modification 11

4.2 Groundwater Flow Simulations 12

4.3 Particle Tracking 12

4.4 Radionuclide Transport 13

4.5 Sensitivity Analysis 16

4.6 Code Execution and Run Control 16

4.6.1 Flow 17

4.6.2 Transport 19

5.0 RESULTS 21

5.1 Flow 21

5.2 Particle Tracking 22

5.3 Radionuclide Transport 29

5.4 Sensitivity Analysis 54

Information Only

6.0 SUMMARY 60

7.0 REFERENCES 61

8.0 APPENDIX A – NO-MINING RESULTS 64

8.1 Flow 64

8.2 Particle Tracking 65

8.3 References 67

Information Only

LIST OF FIGURES

Figure 1. Schematic of Dual Porosity Model....4
Figure 2. Culebra Modeling Domain....6
Figure 3. Culebra Release Point Locations....8
Figure 4. Mining Scenarios and Mass Release Points....10
Figure 5. Culebra Flow Model Run Control Diagram....18
Figure 6. Culebra Transport Model Run Control Diagram....20
Figure 7. Ensemble Mean Flow Rate....22
Figure 8. DTRKMF Particle Travel Time to LWB: CRA-2026 Versus RPPCR....24
Figure 9. DTRKMF Particle Tracks....25
Figure 10. Particle Travel Time to LWB Exceedance Probabilities....26
Figure 11. Mass Breakthrough at 10,000-yr: CRA-2026 Versus RPPCR Full Mining Scenario..32
Figure 12. Mass Breakthrough at 10,000-yr: CRA-2026 Versus RPPCR Partial Mining Scenario....33
Figure 13. Mass Breakthrough Over Time: CRA-2026 Versus RPPCR Full Mining Scenario....34
Figure 14. Mass Breakthrough Over Time: CRA-2026 Versus RPPCR Partial Mining Scenario 35
Figure 15. Exceedance Probability of ^{241}Am Mass to LWB in 10,000 Years....36
Figure 16. Exceedance Probability of ^{23A}Th Mass to LWB in 10,000 Years....37
Figure 17. Exceedance Probability of ^{239}Pu Mass to the LWB in 10,000 Years....38
Figure 18. Exceedance Probability of ^{234}U Mass to LWB in 10,000 Years....39
Figure 19. Exceedance Probability of ^{230}Th Mass to LWB in 10,000 Years....40
Figure 20. DTRKMF particle travel time to LWB versus mining factor....59
Figure 21. Ensemble Mean Flow Rate for the No-Mining Scenario....64
Figure 22. DTRKMF Particle Tracks and Travel Time to LWB Exceedance Probabilities....66

Information Only

LIST OF TABLES

Table 1. Location of Culebra Release Point 2 2
Table 2. Culebra Model Domain Coordinates 5
Table 3. Culebra Release Point Coordinates....7
Table 4. Culebra Flow Uncertain Parameter Distributions....12
Table 5. Deterministic Physical Parameter Values....13
Table 6. Uncertain Physical Parameter Distributions 14
Table 7. Deterministic Chemical Parameter Values 15
Table 8. Uncertain Chemical Parameter distributions 15
Table 9. Mean Particle Travel Time [yr] to LWB for Full Mining Scenario 27
Table 10. Median Particle Travel Time [yr] to LWB for Full Mining Scenario 27
Table 11. Minimum Particle Travel Time [yr] to LWB for Full Mining Scenario 27
Table 12. Maximum Particle Travel Time [yr] to LWB for Full Mining Scenario....28
Table 13. Mean Particle Travel Time [yr] to LWB for Partial Mining Scenario 28
Table 14. Median Particle Travel Time [yr] to LWB for Partial Mining Scenario 28
Table 15. Minimum Particle Travel Time [yr] to LWB for Partial Mining Scenario 29
Table 16. Maximum Particle Travel Time [yr] to LWB for Partial Mining Scenario....29
Table 17. Mean Cumulative Mass [kg] of ^{241}Am to LWB for Full Mining Scenario 41
Table 18. Median Cumulative Mass [kg] of ^{241}Am to LWB for Full Mining Scenario 41
Table 19. Maximum cumulative mass [kg] of ^{241}Am to LWB for Full Mining Scenario 41
Table 20. Mean Cumulative Mass [kg] of ^{241}Am to LWB for Partial Mining Scenario 42
Table 21. Median Cumulative Mass [kg] of ^{241}Am to LWB for Partial Mining Scenario 42
Table 22. Maximum Cumulative Mass [kg] of ^{241}Am to LWB for Partial Mining Scenario....42
Table 23. Mean Cumulative Mass [kg] of ^{239}Pu to LWB for Full Mining Scenario 43
Table 24. Median Cumulative Mass [kg] of ^{239}Pu to LWB for Full Mining Scenario 43
Table 25. Maximum Cumulative Mass [kg] of ^{239}Pu to LWB for Full Mining Scenario....43
Table 26. Mean Cumulative Mass [kg] of ^{239}Pu to LWB for Partial Mining Scenario 44
Table 27. Median Cumulative Mass [kg] of ^{239}Pu to LWB for Partial Mining Scenario 44
Table 28. Maximum Cumulative Mass [kg] of ^{239}Pu to LWB for Partial Mining Scenario....44
Table 29. Mean Cumulative Mass [kg] of ^{23A}Th to LWB for Full Mining Scenario 45

Information Only

Table 30. Median Cumulative Mass [kg] of ^{23A}Th to LWB for Full Mining Scenario 45
Table 31. Maximum Cumulative Mass [kg] of ^{23A}Th to LWB for Full Mining Scenario.....45
Table 32. Mean Cumulative Mass [kg] of ^{23A}Th to LWB for Partial Mining Scenario 46
Table 33. Median Cumulative Mass [kg] of ^{23A}Th to LWB for Partial Mining Scenario 46
Table 34. Maximum Cumulative Mass [kg] of ^{23A}Th to LWB for Partial Mining Scenario.....46
Table 35. Mean Cumulative Mass [kg] of ^{234}U to LWB for Full Mining Scenario 47
Table 36. Median Cumulative Mass [kg] of ^{234}U to LWB for Full Mining Scenario 47
Table 37. Maximum Cumulative Mass [kg] of ^{234}U to LWB for Full Mining Scenario.....47
Table 38. Mean Cumulative Mass [kg] of ^{234}U to LWB for Partial Mining Scenario 48
Table 39. Median Cumulative Mass [kg] of ^{234}U to LWB for Partial Mining Scenario 48
Table 40. Maximum Cumulative Mass [kg] of ^{234}U to LWB for Partial Mining Scenario.....48
Table 41. Mean Cumulative Mass [kg] of ^{230}Th to LWB for Full Mining Scenario.....49
Table 42. Median Cumulative Mass [kg] of ^{230}Th to LWB for Full Mining Scenario.....49
Table 43. Maximum Cumulative Mass [kg] of ^{230}Th to LWB for Full Mining Scenario 49
Table 44. Mean Cumulative Mass [kg] of ^{230}Th to LWB for Partial Mining Scenario.....50
Table 45. Median Cumulative Mass [kg] of ^{230}Th to LWB for Partial Mining Scenario.....50
Table 46. Maximum Cumulative Mass [kg] of ^{230}Th to LWB for Partial Mining Scenario 50
Table 47. Cumulative Mass to LWB [Count > 10^{-9} kg] of ^{241}Am for Full Mining Scenario 51
Table 48. Cumulative Mass to LWB [Count > 10^{-9} kg] of ^{241}Am for Partial Mining Scenario 51
Table 49. Cumulative Mass to LWB [Count > 10^{-9} kg] of ^{239}Pu for Full Mining Scenario 51
Table 50. Cumulative Mass to LWB [Count > 10^{-9} kg] of ^{239}Pu for Partial Mining Scenario 52
Table 51. Cumulative Mass to LWB [Count > 10^{-9} kg] of ^{234}U for Full Mining Scenario 52
Table 52. Cumulative Mass to LWB [Count > 10^{-9} kg] of ^{234}U for Partial Mining Scenario 52
Table 53. Cumulative Mass to LWB [Count > 10^{-9} kg] of ^{23A}Th for Full Mining Scenario 53
Table 54. Cumulative Mass to LWB [Count > 10^{-9} kg] of ^{23A}Th for Partial Mining Scenario 53
Table 55. Cumulative Mass to LWB [Count > 10^{-9} kg] of ^{230}Th for Full Mining Scenario.....53
Table 56. Cumulative Mass to LWB [Count > 10^{-9} kg] of ^{230}Th for Partial Mining Scenario.....54
Table 57. Stepwise Ranked Regression of ^{241}Am for CRA-2026 CRP 2 Full Mining Scenario...55
Table 58. Stepwise Ranked Regression of ^{241}Am for RPPCR CRP 2 Full Mining Scenario.....56
Table 59. Stepwise Ranked Regression of ^{239}Pu for CRA-2026 CRP 2 Full Mining Scenario 56

Information Only

Table 60. Stepwise Ranked Regression of ^{239}Pu for RPPCR CRP 2 Full Mining Scenario 57
Table 61. Stepwise Ranked Regression of ^{234}U for CRA-2026 CRP 2 full mining scenario.....57
Table 62. Stepwise Ranked Regression of ^{234}U for RPPCR CRP 2 Full Mining Scenario.....58
Table 63. Stepwise Ranked Regression of ^{23A}Th for CRA-2026 CRP 2 Full Mining Scenario....58
Table 64. Stepwise Ranked Regression of ^{23A}Th for RPPCR CRP 2 Full Mining Scenario.....59
Table 65. Particle Travel Time [yr] to LWB Statistics for the No-Mining Scenario 67

Information Only

1.0 INTRODUCTION

The Waste Isolation Pilot Plant (WIPP), located in southeastern New Mexico, has been developed by the U.S. Department of Energy (DOE) for the geologic disposal of transuranic (TRU) waste. The containment of TRU waste at WIPP is regulated by the U.S. Environmental Protection Agency (EPA) under Title 40 of the Code of Federal Regulations (CFR), Part 191.

The DOE demonstrates compliance with the containment requirements of 40 CFR 191.13 by means of performance assessment (PA) as described in the Certification Criteria of Title 40 CFR Part 194. Sandia National Laboratories (SNL) conducts PAs at the request of the DOE. The PA calculations estimate the probability and consequences of potential radionuclide releases from the repository to the accessible environment over a regulatory period of 10,000 years following facility closure. The PA models are continuously maintained and updated with new information, which typically leads to refinements and modifications in both the models and their parameters. Additionally, planned changes to the repository and its components necessitate updates to the WIPP PA models.

All previous WIPP certifications have been based on a repository consisting of 10 panels. In March 2024, the DOE submitted the Replacement Panels Planned Change Request (RPPCR) to seek EPA approval for waste emplacement in two new panels, referred to as replacement panels, located to the west of the existing operations area (Bollinger 2024). The EPA approved the RPPCR in July 2025 (U.S. EPA 2025).

The addition of the two replacement panels is not expected to provide adequate space for the disposal of the allowable waste volume designated for WIPP under the Land Withdrawal Act (LWA); thus, the 12-panel configuration is regarded as an interim state of the repository. The DOE may pursue approval for waste disposal in seven additional panels to accommodate the full allowable volume of waste. This hypothetical 19-panel configuration is considered the anticipated final state of the repository.

The RPPCR considered the anticipated final state of the repository, which includes a total of 19 waste panels, the total allowable inventory volume, and represented releases to the Culebra with four mass release points. The CRA-2026 12-panel configuration incorporates two mass release points, and the 19-panel configuration employs four. Three of these release points are common with those of the RPPCR. The release point location over the additional replacement panels is consistent between the interim and final state repository configurations but is shifted from that used in the RPPCR. This change created small differences between the RPPCR and CRA-2026 final and interim state Culebra flow and radionuclide transport results. This report analyzes all four mass release points, encompassing Culebra flow and radionuclide transport components of the CRA-2026 PA for both the interim and final state repositories. Changes since the RPPCR are documented by comparing the CRA-2026 results to the RPPCR.

The CRA-2026 is the fifth recertification application for the WIPP submitted by the DOE for EPA approval. The PA executed by SNL in support of the CRA-2026 PA is described in AP-214 (Hansen et al. 2025).

Information Only

2.0 CHANGES SINCE THE RPPCR

Changes incorporated into the CRA-2026 PA relative to the RPPCR that impact Culebra Flow and transport results include:

- The location of the Culebra release point (CRP) for the replacement waste panels.

Inventory parameters are not incorporated into the Culebra flow or transport models. The change listed above is discussed in more detail in the sections that follow.

2.1 Culebra Release Point Location

For the RPPCR, the Culebra release point 2 (CRP 2) was located at the centroid of Panels 11, 12, and 13 in a 19-panel representation of the WIPP repository. For the interim state repository with only Panels 11 and 12, CRP 2 is located at the centroid of Panels 11 and 12 (Wilgus and Brunell 2025). The updated coordinates are shown in Table 1. The same CRP 2 location is used for the 19-panel final state repository. The locations of the other Culebra Release Points (CRP 1, CRP 3, and CRP 4) remain unchanged.

Table 1. Location of Culebra Release Point 2

Analysis	UTM (x)	UTM (y)	SECO (i)	SECO (j)
RPPCR	612828.31	3581621.38	52	81
CRA-2026	612929.61	3581621.38	54	81

2.2 Parameters Not Updated as Anticipated in Analysis Plan AP-214

AP-214 (Hansen et al. 2025) indicates that several parameters were expected to be updated for CRA-2026. Specifically, the parameter specifying the likelihood of low or high oxidation state for an actinide (property OXCUTOFF for materials NP, PU, and U) and the parameters related to mineral and intrinsic colloids (properties CONCMIN and CONCINT for materials AM, NP, PU, TH, and U) were anticipated to undergo revisions. Kaplan et al. (2025) re-examines the basis for these parameter values and recommends the continued use of the RPPCR values. As a result, no changes were made to these parameters for CRA-2026. The only parameters in this report that would be impacted by these updates would be property OXCUTOFF for materials PU and U.

Information Only

3.0 CONCEPTUAL APPROACH

The Culebra flow and transport models implement the WIPP conceptual models for Culebra Hydrogeology and Transport of Dissolved Actinides in the Culebra, and in part the conceptual model for Transport of Colloidal Actinides in the Culebra (Holt 1997; Hart et al. 2008; Burgess et al. 2008; McCormick et al. 2024). No changes have been made to the conceptualization of Culebra flow and transport models since the RPPCR PA.

The Culebra Dolomite Member of the Rustler Formation has been identified as the most transmissive saturated unit above the Salado Formation and consequently it is the most likely subsurface release pathway of radionuclides to the LWB. Radionuclide movement through the Culebra is a function of the groundwater flow-field and the transport properties of the media and radionuclide species being considered. Flow occurs through fractures, vugs and, to some extent, intergranular pores. There is a large permeability contrast (up to 10 orders of magnitude) between the different scales of interconnected porosity that suggests a dual porosity conceptualization consisting of advective porosity (i.e., fracture porosity) and diffusive porosity (i.e., matrix porosity; Figure 1). Tracer tests conducted in the Culebra at the WIPP site have clearly shown characteristics of both advective transport and matrix diffusion (Meigs et al. 2000).

Information Only

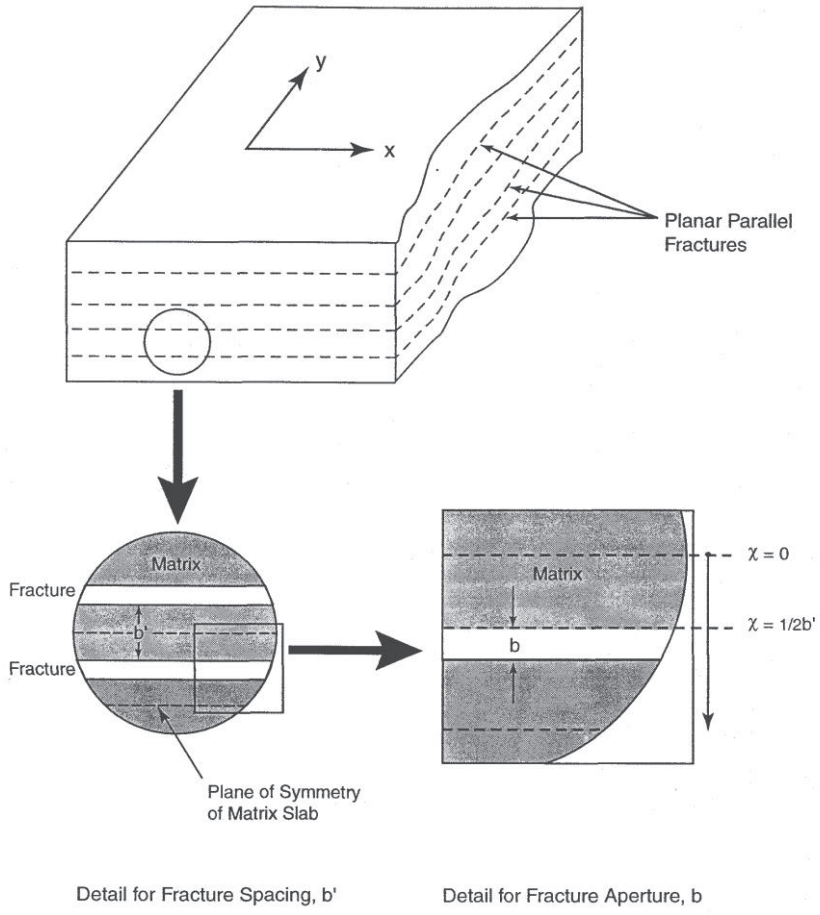

Figure 1. Schematic of Dual Porosity Model

Potash mining in the vicinity of the WIPP involves resource extraction below the Culebra Dolomite Member in the McNutt Potash zone, a subsection of the Salado Formation that is above the repository horizon but below the Rustler Formation. It is hypothesized that subsidence of the Culebra due to potash mining leads to fracturing, resulting in higher Culebra transmissivities and altered groundwater flow patterns. This increase in transmissivity may significantly change the transport behavior of any radionuclides entering the aquifer via human intrusion from the underlying repository.

3.1 Domain and Discretization

The Culebra flow and transport model domain and discretization are the same as in the RPPCR calculations (Kuhlman 2010). The flow model domain is a two-dimensional horizontal layer that extends 28.4 kilometers in the east-west direction and 30.7 kilometers in the north-south direction (Table 2; Figure 2). The flow domain is aerially discretized into 100-meter square cells, yielding

Information Only

a model that is 284 cells wide (east-west) by 307 cells tall (north-south). The flow domain is vertically discretized into a single horizontal layer of uniform 7.75-meter thickness. The transport model domain is a 7.5-kilometer by 5.4-kilometer subregion of the flow domain that encompasses the southern extent of the LWB. The transport domain is shifted off-center in the north-south direction because the undisturbed groundwater flow direction is generally north to south. The transport domain is discretized into 50-meter grid cells that are created by bisecting the Culebra 100-m flow model cells on both the x and y axes. Although the Culebra properties vary in the vertical direction, the error introduced by modeling the Culebra in two rather than three dimensions has been determined to be negligible (Corbet 1995).

Table 2. Culebra Model Domain Coordinates

Domain Corner	X Coordinate [A] [m]	Y Coordinate [A] [m]
Flow Model Domain		
Northeast	630,000	3,597,100
Northwest	601,700	3,597,100
Southwest	601,700	3,566,500
Southeast	630,000	3,566,500
WIPP Land Withdrawal Boundary		
Northeast	616,941	3,585,109
Northwest	610,495	3,585,068
Southwest	610,567	3,578,623
Southeast	617,015	3,578,681
Transport Model Domain		
Northeast	617,750	3,583,000
Northwest	610,250	3,583,000
Southwest	610,250	3,577,600
Southeast	617,750	3,577,600

[A] UTM NAD27 Zone 13 N

Information Only

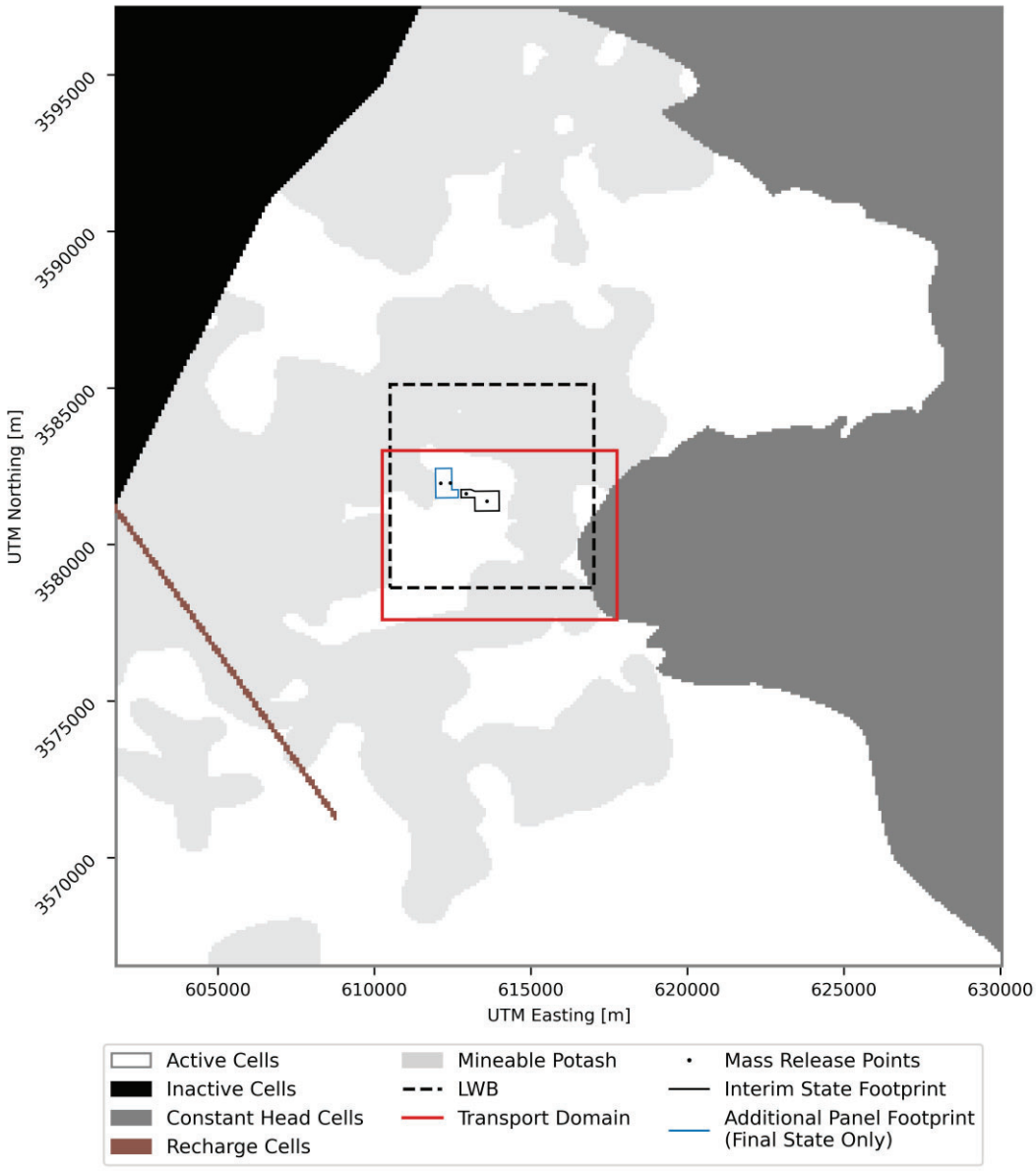

Figure 2. Culebra Modeling Domain

Other key model domain features shown in Figure 2 include no flow (inactive cells) and constant head boundaries (see section 3.2) as well as recharge cells (Kuhlman 2010), and extent of mineable potash (Cranston 2009).

In each simulation, the Culebra transport model includes mass release into the Culebra at one of four discrete Culebra release points (CRPs) above the waste panels (Figure 2). The UTM NAD27 Zone 13N coordinates of the release points are listed in Table 3. CRP locations were determined by characterizing potential particle travel pathways and times across the flow domain (Kushnereit

Information Only

et al. 2020) and subsequently grouping panels with similar behavior (Bethune and Brunell 2022; Figure 3, modified from Sjomeling 2019). For the CRA-2026, CRP 2 was relocated to the centroid of panels 11 and 12. Consideration of all four mass release points represents the final state of the repository while consideration of CRP 1 and CRP 2 represents the interim state repository. For consistency among release points the same location is used for both the 19-panel and 12-panel repository representations (Wilgus and Brunell 2025). This consistency allows for more direct comparison of results for the 12-panel interim state to those of the 19-panel final state PA.

Table 3. Culebra Release Point Coordinates

Culebra Release Point	X-Coordinate [m]	Y-Coordinate [m]	Description
CRP 1	613597.5	3581385.2	Centroid of panels 1 through 10, within CRP 1 panel area
CRP 2	612929.6	3581621.4	Centroid of panels 11 and 12, within CRP 2 panel area
CRP 3	612424.1	3581961.0	Centroid of panels 14 and 19, within CRP 3 panel area
CRP 4	612120.2	3581957.6	Centroid of panels 15 through 18, within CRP 3 panel area

Information Only

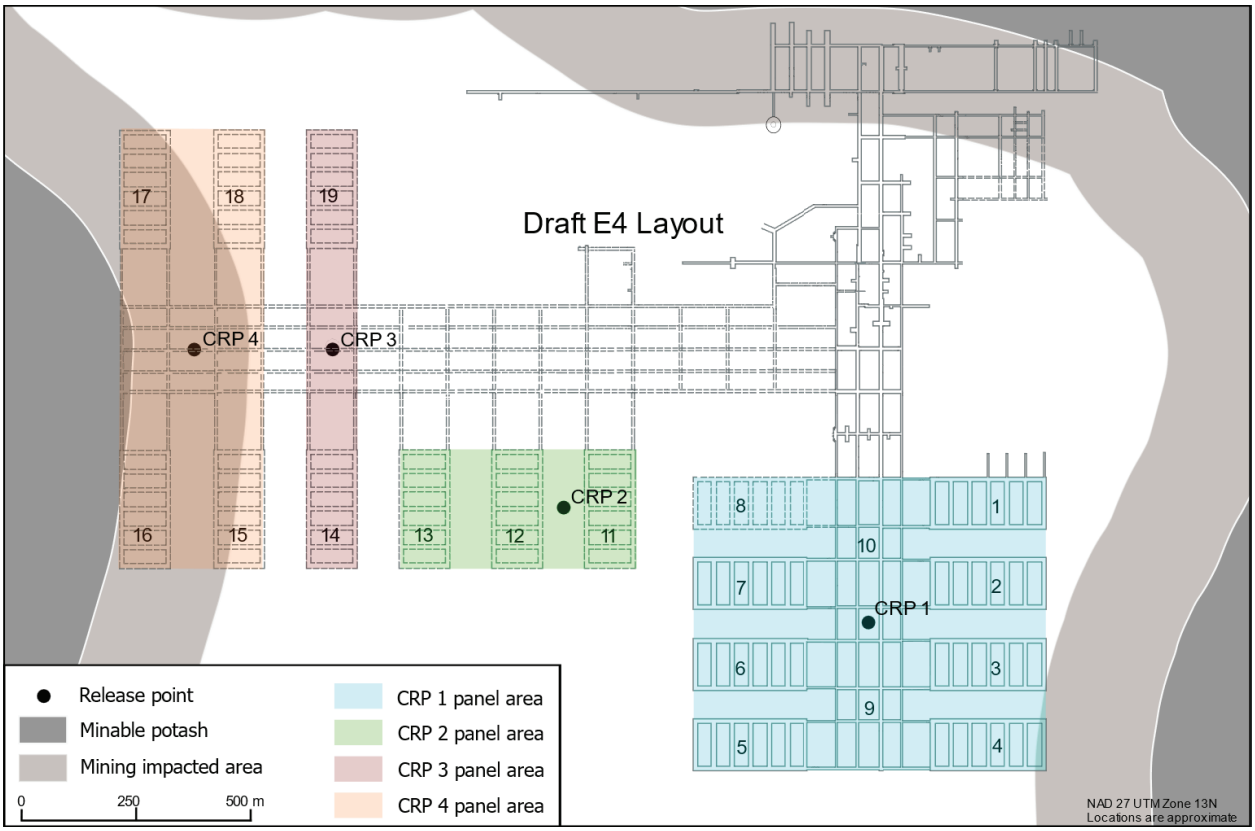

Figure 3. Culebra Release Point Locations

3.2 Boundary and Initial Conditions

The constant-head region associated with the halite-sandwiched portion of the Culebra is specified head, set to the land surface elevation. The model boundary conditions along straight-line portions of the north, west, and south edges of the domain are fixed at their initial head values. A multi-parameter parametric surface was used to fill initial head and boundary condition values everywhere except in no-flow cells and in the constant-head zone east of the halite margin (Bowman et al. 2023). The piecewise-linear boundary in the northwest corner is a no-flow boundary parallel to the axis of the Nash Draw topographic depression, which is conceptualized as a groundwater divide.

The regional gradient across the domain is approximately:

(944.14 m – 908.88 m)/30.7 km = 0.00115

as calculated by averaging the constant heads along the non-halite-sandwiched portion of the northern boundary (columns 1 to 140, 944.14 m), subtracting the average heads along the entire southern boundary (908.88-m), and then dividing by the north-south model domain distance (30.7 km).

Information Only

3.3 Uncertainty

There is significant uncertainty associated with characterizing the physical properties of geologic materials that influence Culebra flow and transport behavior. Properties such as permeability and porosity are usually measured indirectly and vary significantly depending upon location and scale. The uncertainty in a particular physical property value is called subjective (epistemic) uncertainty. Stochastic (aleatory) uncertainty is associated with incomplete knowledge of future events. WIPP PA separately addresses both types of uncertainty.

3.3.1 Subjective Uncertainty

Subjective uncertainty is modeled by defining and sampling from distributions that characterize uncertain parameters. Uncertain physical properties in the Culebra flow and transport models are categorized as epistemic. To reduce the number of realizations required and to ensure that low probability (and possibly high consequence) combinations are represented, Latin Hypercube Sampling (LHS) is used to create the realizations. For the WIPP PA, the LHS software is used to create 100 distinct parameter sets, or vectors, that are sampled from the full range of parameter uncertainty (WIPP PA 2021). To ensure that the Latin Hypercube parameter sets are representative and mean releases are convergent, three replicates are created for a total of 300 separate vectors.

3.3.2 Stochastic Uncertainty

Stochastic uncertainty is addressed in the PA by generating 10,000 random sequences of future events, termed futures, using the WIPP PA software program CCDFGF. To estimate releases by Culebra transport in a random future, radionuclide transport is calculated for defined scenarios and these scenario results are used to construct the releases for all future events.

Two aspects of the Culebra flow and transport model are addressed through defined scenarios, including potash mining impacts on flow, and the location of future drilling events. Two mining scenarios are considered: full mining, in which mining is assumed in all economically feasible potash reserves throughout the domain, and partial mining, in which mining is assumed to occur only outside the LWB (Figure 4). Since the potash-mining horizon is below the Culebra, the areas in the Culebra that are disturbed by mining activities in the Salado are larger than the mined areas due to angle-of-draw effects, in which the subsidence effects are assumed to propagate up and out at 45° angles from horizontal. Consideration of this propagation in map view defines the mining impacted areas which extend ~300 m beyond the mineable potash area (Figure 3). Uncertainty in the location of future drilling events that could potentially connect the Culebra with the repository waste region is addressed by modeling mass release into the Culebra at four different release point locations, termed CRP 1 through CRP 4. Transport is evaluated for each combination of mining scenario and release point (Figure 4).

Information Only

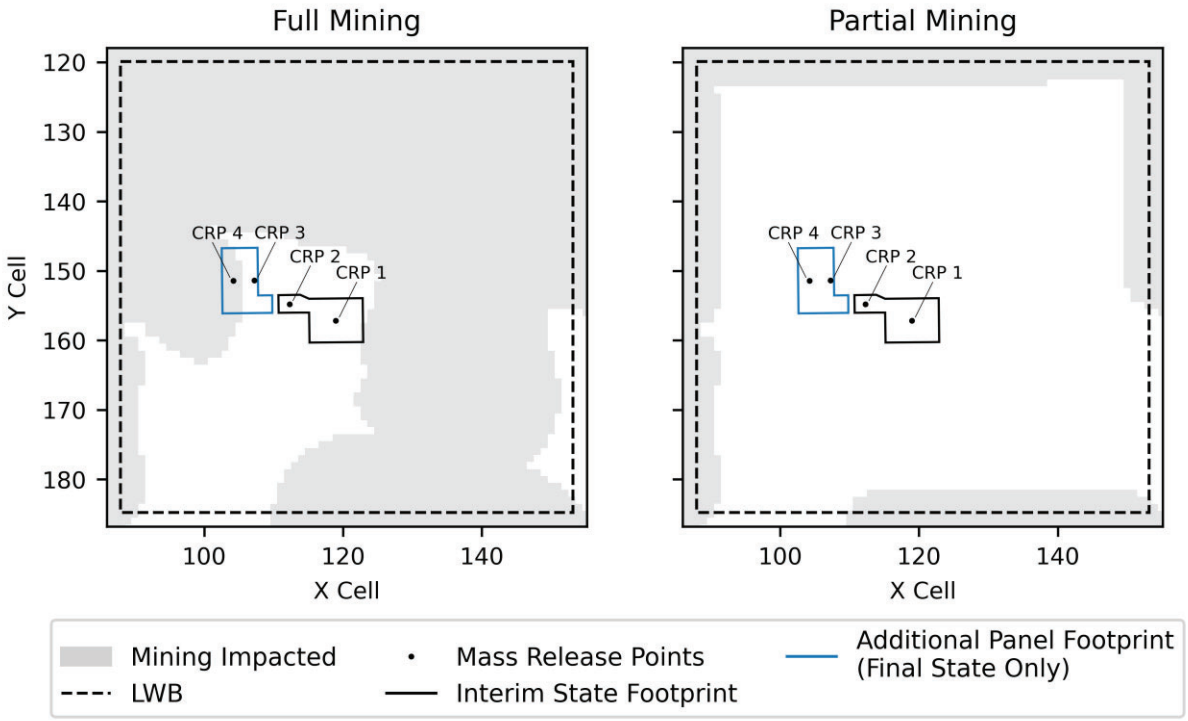

Figure 4. Mining Scenarios and Mass Release Points

Information Only

4.0 CULEBRA MODEL METHODOLOGY

The primary result of interest in the Culebra transport calculations is the cumulative transport of radionuclides to the LWB over the 10,000-year regulatory period, conditional on sources placed in the Culebra at 50 years post-closure. There are five steps in estimating radionuclide transport through the Culebra, including:

Step 1. Construction of 1,000 base geostatistical realizations of Culebra hydraulic transmissivity (T), anisotropy, storativity, and recharge fields (collectively referred to as "T-fields");

Step 2. Calibration of the T-fields to observed head and pumping drawdowns including selection of a final set of the 100 best fit realizations;

Step 3. Modification of the T-fields to account for potential subsidence due to potash mining beneath the Culebra;

Step 4. Calculation of steady-state groundwater flow-fields for each mining-modified T-field using MODFLOW6; and

Step 5. Calculation of radionuclide transport through the Culebra to the LWB for each simulated flow-field and release location using SECOTP2D.

Step 1 is documented in Hart et al. (2008). Step 2 is documented in Bowman et al. (2023). Steps 1 and 2 produce 100 equally likely T-fields that are input to Step 3. The work presented in this report is limited to Step 3 through Step 5. The output of Step 5 is used by the WIPP software CCDFGF to calculate potential radionuclide releases through the Culebra to the accessible environment (King et al. 2025).

4.1 Mining Modification

The calibrated transmissivity fields are modified into the two mining scenarios with the scripts *enlarge_mining_areas.py* and *mining_mod.py*. The script *enlarge_mining_areas.py* enlarges the mining regions to account for the angle of draw and identifies the mining impacted cells within the LWB. The script *mining_mod.py* modifies the calibrated transmissivity fields in the mining impacted regions.

WIPP PA Parameter Database (PAPDB) designations for the parameters involved in the mining modification calculation are shown in Table 4. The parameter MINP_FAC is a multiplier on the transmissivity values that controls the degree of impact of mining. The parameter TRANSIDX is used as an index to create a random pairing between calibrated T-field realizations with LHS vectors. Each vector in the CRA-2026 has the same LHS values and the same T-field index value as in the RPPCR (King and Zeitler 2025).

Information Only

Table 4. Culebra Flow Uncertain Parameter Distributions

Model Parameter	MATERIAL: PROPERTY	Units	Distribution	Range	Median
Flow-field index	GLOBAL:TRANSIDX	-	Uniform	[0.00E+0, 1.00E+0]	0.50
Mining factor	CULEBRA:MINP_FAC	-	Uniform	[1.00E+0, 1.00E+3]	500.5

4.2 Groundwater Flow Simulations

MODFLOW6 simulates steady-state flow with the mining-modified transmissivity fields at two resolutions:

1) 100-m grid used in the T-field calibrations and particle tracking simulations
2) 50-m grid used in the mass transport simulations

The flow model is converted to 50×50-meter grid cells by subdividing each of the 100-meter model grid cells into four equal-sized cells with the properties of the larger cells copied directly into the smaller cells. Copied properties include the boundary condition data fields for, top and bottom elevation arrays, the starting head array, and the T-fields input anisotropy, mining modified conductivity, recharge, and storage using the script *100x100m_to_50x50m.py*. The boundary condition head values are smoothed along the exterior two rows and columns of the domain.

4.3 Particle Tracking

DTRKMF tracks a single, non-sorbing particle through the simulated flow fields to the LWB for each combination of release point, transmissivity field, parameter vector, and mining scenario. During the RPPCR a problem was found in DTRKMF version 1.02 (WIPP PA 2020) that could potentially cause a particle track to get stuck, then suddenly jump in an unrealistic way (WIPP PA 2023). This issue was resolved in DTRKMF version 2.00 (WIPP PA 2024a; WIPP PA 2024b).

Results are then summarized into text tables with the script *summarize_dtrkmf.py*. Consistent with the RPPCR, diffusive porosity (CULEBRA:DPOROS) was set to 16%, and the particle travel times tabulated in the summary files were multiplied by the factor 4.0/7.75. This factor adjusts the values from the 7.75-meter thickness of the Culebra used in the MODFLOW6 flow simulations to the 4.0-meter transport thickness used in the transport simulations (Holt 1997; Kuhlman 2010).

Particle tracking output is used to index the flow fields by travel time to the LWB for the sensitivity analysis. Particle tracking output also allows for visualization and quantification of the flow characteristics from each of the Culebra release points to the LWB. Particle tracking results do not take into consideration retardation, dispersion, or molecular diffusion.

Information Only

4.4 Radionuclide Transport

Mass transport is simulated with the WIPP PA software SECOTP2D assuming parallel plate fracturing where fluid flow is restricted to the advective continuum (fractures), and mass is transferred between the advective and diffusive (matrix) continua via molecular diffusion (Figure 1). Retardation is implemented in the diffusive domain assuming linear equilibrium isotherms defined with a matrix distribution coefficient for each species. Radioactive decay is implemented with multiple straight decay chains. Only flow velocity is spatially distributed in the Culebra transport model; other quantities (e.g. advective/diffusive porosity) are implemented as constant values over the entire spatial extent for each simulation.

The transport preprocessing program PRESECOTP2D performs several transformations to prepare the MODFLOW6 50-m cell-by-cell flow output for the transport simulations, including performing basic coordinate system transformations, windowing into the transport subdomain, converting the volumetric flow rates to the vertical thickness of 4.0 m to focus all flow through the more permeable portion of the Culebra, and multiplying the volumetric flow rates by the LHS sampled climate factor parameter.

In each transport simulation, 1 kg of each of four radionuclides is released at one of the four release points during the first 50 years after repository closure. The radionuclides transported in the Culebra are ^{241}Am, ^{239}Pu, ^{230}Th, and ^{234}U. Transport of the ^{230}Th daughter product of ^{234}U decay is calculated and tracked as a separate species. Throughout this document, ^{230}Th will refer to the ^{234}U daughter product and ^{23A}Th will refer to the ^{230}Th released at the release point. The cumulative fraction of the mass that crosses the LWB is then tabulated at 50-year intervals for each radionuclide.

The PAPDB designations for the deterministic and uncertain physical transport parameters are shown in Table 5 and Table 6, respectively. These parameter values have not changed since the CCA. Advective and diffusive porosity and matrix half-block length are used in the dual-domain mass transport equations. The climate index parameter is used to scale the computed mining-modified flow velocity to account for the potential impact of climate change (Corbet and Swift 1996). For uncertain quantities, one sampled value is used to specify a particular parameter value over its entire spatial extent in a single realization.

Table 5. Deterministic Physical Parameter Values

Model Parameter	MATERIAL: PROPERTY	Units	Value
Longitudinal dispersivity	CULEBRA:DISP_L	m	0
Transverse dispersivity	CULEBRA:DISPT_L	m	0
Fracture tortuosity	CULEBRA:FTORT	-	1.0
Diffusive tortuosity	CULEBRA:DTORT	-	0.11
Skin resistance	CULEBRA:SKIN_RES	-	0
Material grain density	CULEBRA:DNSGRAIN	kg/m^3	2820

Information Only

Table 6. Uncertain Physical Parameter Distributions

Model Parameter	MATERIAL: PROPERTY	Units	Distribution	Range	Median
Advective porosity	CULEBRA:APOROS	-	Log-uniform	[1.00E-4, 1.00E-2]	0.001
Diffusive porosity	CULEBRA:DPOROS	-	Cumulative	[1.00E-1, 2.50E-1]	0.160
Matrix half-block length	CULEBRA:HMBLKLT	m	Uniform	[5.00E-2, 5.00E-1]	0.275
Climate index	GLOBAL:CLIMTIDX	-	Cumulative	[1.00E+0, 2.25E+0]	1.170

The PAPDB designations for the deterministic and uncertain chemical transport parameters are shown in Table 7 and Table 8, respectively. Actinides Pu and U may be present in high or low oxidation states, with separate matrix distribution coefficient parameter distributions and molecular diffusion values defined for each. The parameter OXSTAT is used to determine oxidation state. In the RPPCR two constant parameters defined actinide-specific thresholds of the OXSTAT value to determine the actinide oxidation state. The oxidation cutoff for U results in 50% likelihoods of U(IV) or U(VI), while the oxidation cutoff for Pu results in a 25% likelihood of Pu(III) and a 75% likelihood of Pu(IV). The actinide oxidation state approach in CRA-2026 is the same as the RPPCR (see Section 2.3).

Information Only

Table 7. Deterministic Chemical Parameter Values

Species	Model Parameter	MATERIAL: PROPERTY	Units	Value
^{241}Am	Atomic Weight	AM241:ATWEIGHT	kg/mole	2.411E-01
^{241}Am	Half-life	AM241:HALFLIFE	s	1.364E+10
^{241}Am	Molecular Diffusion	AM+3:MD0	[m^2/s]	3.00E-10
^{239}Pu	Atomic Weight	PU239:ATWEIGHT	kg/mole	2.391E-01
^{239}Pu	Half-life	PU239:HALFLIFE	s	7.594E+11
^{239}Pu	Oxidation state threshold	PU:OXCUTOFF	-	0.25
^{239}Pu	Molecular Diffusion	PU+3:MD0	[m^2/s]	3.00E-10
^{239}Pu	Molecular Diffusion	PU+4:MD0	[m^2/s]	1.53E-10
^{230}Th	Atomic Weight	TH230:ATWEIGHT	kg/mole	2.300E-01
^{230}Th	Half-life	TH230:HALFLIFE	s	2.430E+12
^{230}Th	Molecular Diffusion	TH+4:MD0	[m^2/s]	1.53E-10
^{234}U	Atomic Weight	U234:ATWEIGHT	kg/mole	2.340E-01
^{234}U	Half-life	U234:HALFLIFE	s	7.716E+12
^{234}U	Oxidation state threshold	U:OXCUTOFF	-	0.50
^{234}U	Molecular Diffusion	U+4:MD0	[m^2/s]	1.53E-10
^{234}U	Molecular Diffusion	U+6:MD0	[m^2/s]	4.26E-10

Table 8. Uncertain Chemical Parameter distributions

Model Parameter	MATERIAL: PROPERTY	Units	Distribution	Range	Median
Oxidation state index	GLOBAL:OXSTAT	-	Uniform	[0.00E+0, 1.00E+0]	0.50
Matrix distribution coefficient					
Am(III)	AM+3:MKD_AM	m^3/kg	Log-uniform	[5.00E-3, 4.00E-1]	4.50E-2
Pu(III)	PU+3:MKD_PU	m^3/kg	Log-uniform	[5.00E-3, 4.00E-1]	4.50E-2
Pu(IV)	PU+4:MKD_PU	m^3/kg	Log-uniform	[5.00E-4, 1.00E+1]	7.10E-2
Th(IV)	TH+4:MKD_TH	m^3/kg	Log-uniform	[5.00E-4, 1.00E+1]	7.10E-2
U(IV)	U+4:MKD_U	m^3/kg	Log-uniform	[5.00E-4, 1.00E+1]	7.10E-2
U(VI)	U+6:MKD_U	m^3/kg	Log-uniform	[3.00E-5, 2.00E-2]	7.70E-4

Information Only

4.5 Sensitivity Analysis

The WIPP program STEPWISE is used to determine the relative influence of the sampled parameters on the uncertainty in the output mass discharge to the LWB. STEPWISE performs a stepwise multiple regression analysis on the ranked dependent and independent variables. For the Culebra transport analysis, the cumulative mass transport to the LWB at 10,000 years post-closure is the dependent variable. Independent variables include the following uncertain physical parameter values sampled by LHS (Table 6):

- GLOBAL:CLIMTIDX
- CULEBRA:APOROS
- CULEBRA:DPOROS
- CULEBRA:HMBLKLT

In the RPPCR sensitivity analysis, parameters CULEBRA:APOROS and CULEBRA:DPOROS were referred to as FPOROS (fracture porosity) and MPOROS (matrix porosity) respectively (Table 6).

Independent variables include the matrix distribution coefficients:

- MKD_L: matrix distribution coefficient for each isotope *L*.

MKD represents the combined LHS samples for the oxidation state dependent matrix distribution coefficient, computed for ^{239}Pu as:

$$MKD_PU_v = \begin{cases} PU+3 : MKDPU_v \; if \; GLOBAL:OXSTAT_v \leq PU:OXCUTOFF \\ PU+4 : MKDPU_v \; if \; GLOBAL:OXSTAT_v > PU:OXCUTOFF \end{cases}$$

and for ^{234}U as: $MKD_U_v = \begin{cases} U+4 : MKDU_v \; if \; GLOBAL:OXSTAT_v \leq U:OXCUTOFF \\ U+6 : MKDU_v \; if \; GLOBAL:OXSTAT_v > U:OXCUTOFF \end{cases}$

In these equations, *v* indicates the LHS vector. The PAPDB material and property names are listed in Table 7 and Table 8.

Additionally, particle travel time to the LWB is included as an independent variable representing the variability of the MODFLOW6 flow fields.

- DTRK_TIME: particle travel time to the LWB as a surrogate for flow field impact.

4.6 Code Execution and Run Control

Culebra flow and transport calculations are automated by the WIPP PA Run Control System. Run control diagrams that illustrate the execution order for Culebra flow and transport simulations are provided in Figure 5 and Figure 6, respectively. A full description of the CRA-2026 run control, including names and locations of input and output files, can be found in Long (2025).

CRA-2026 calculations were performed on the WIPP PA HPC/Linux Cluster, which consists of Dell PowerEdge C6420 hardware running CentOS7. The RPPCR calculations were performed on the same system (Long and King 2022; Long 2023; Long 2024).

Information Only

4.6.1 Flow

The run control diagram for flow simulations is shown in Figure 5. Culebra flow simulations were computed with MODFLOW 6, the sixth core release of the groundwater flow software developed by U.S. Geological Survey (Langevin et al. 2017). Further description of MODFLOW 6 input and output is available online at: https://water.usgs.gov/ogw/modflow/mf6io_6.0.3.pdf. In PA, MODFLOW6 software is used in conjunction with several utility programs (GENMESH, MATSET, POSTLHS, SUMMARIZE) which variously set model parameters, material properties, sample from the probability distributions for subjectively uncertain parameters, and write output summary text files.

Several Culebra flow utility scripts were validated under NP 9-1 as documented in the appendices of the Culebra flow and transport analysis report for the RPPCR (Bethune 2023). Appendix A MININGMOD covered *enlarge_mining_areas.py*, *mining_mod.py*, and *100x100_to_50x50.py*. Appendix B SUMMARIZE DTRKMF covers *summarize_dtrkmf.py*. Appendix C CBC2BUD covered the cbc2bud utility while Appendix D covered *bud2text.py*. Execution of these validations remain intact (Long 2025)

CBC2BUD was developed to convert the MODFLOW6 binary cell-by-cell file output to MODFLOW-2000 format compatible with the previous version of particle tracking software, DTRKMF. Since the RPPCR, updates to DTRKMF (version 2; WIPP PA 2024) to optionally read MODFLOW6 output files negate inclusion of CBC2BUD in PA run control.

Information Only

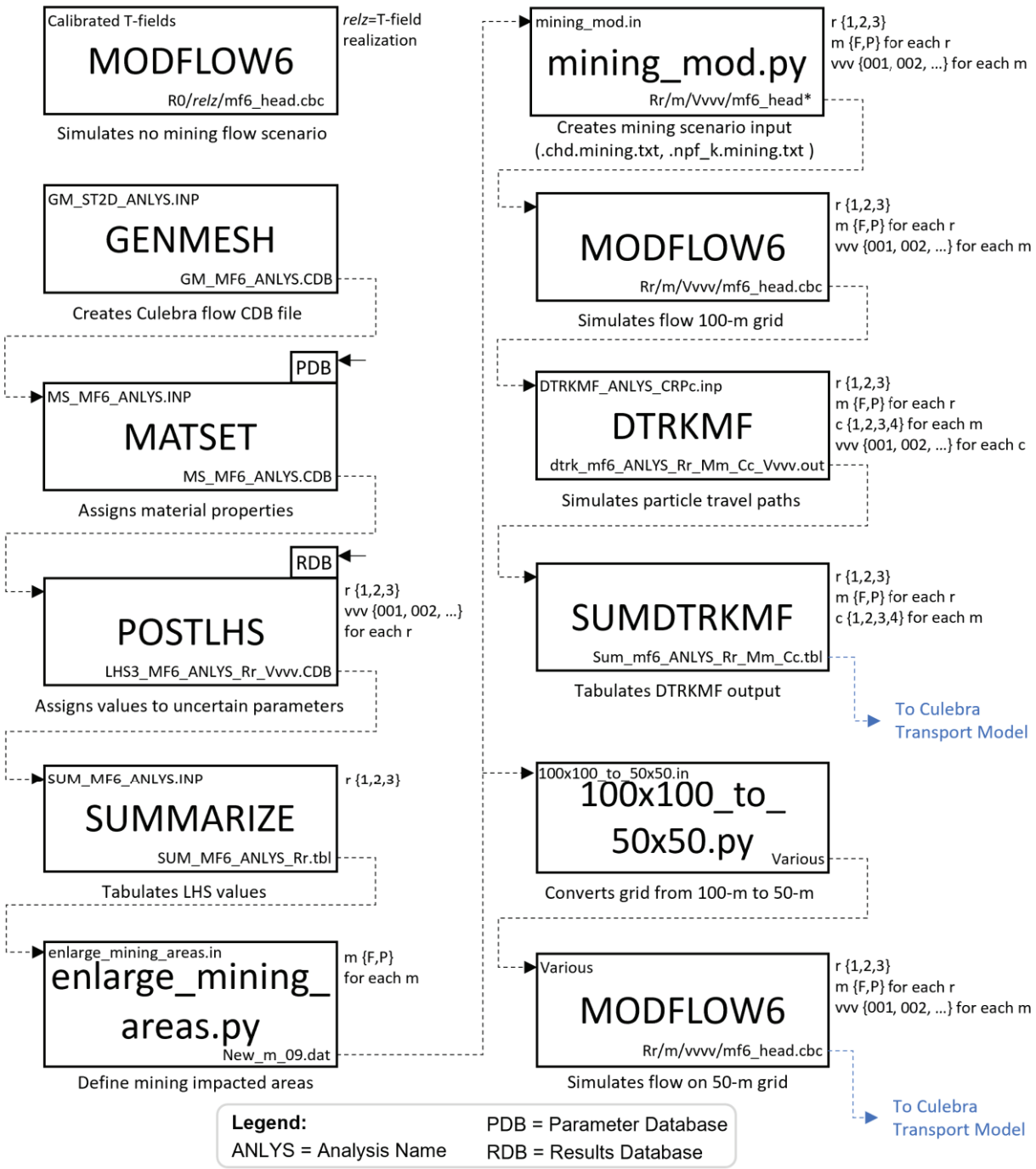

Figure 5. Culebra Flow Model Run Control Diagram

Information Only

4.6.2 Transport

The run control diagram for the transport simulations is shown in Figure 6. The Culebra transport model includes 2,400 calls to the WIPP groundwater transport software SECOTP2D (3 replicates, 2 mining scenarios, 4 mass release points, 100 vectors). The SECOTP2D mass transport simulator is used in conjunction with a preprocessor utility (PRESECOTP2D) and a postprocessor utility (POSTSECOTP2D). In addition, several utility codes are used to sample from the probability distributions for subjectively uncertain parameters, define the mesh, set material properties, and set model parameters. As a part of the Culebra transport model, the STEPWISE software is used to conduct a sensitivity analysis to determine the relative importance of the input parameters in the Culebra transport calculation. The codes used in the transport analysis are qualified per Nuclear Waste Management Procedure NP 19-1: Software Requirements (Long 2024).

Information Only

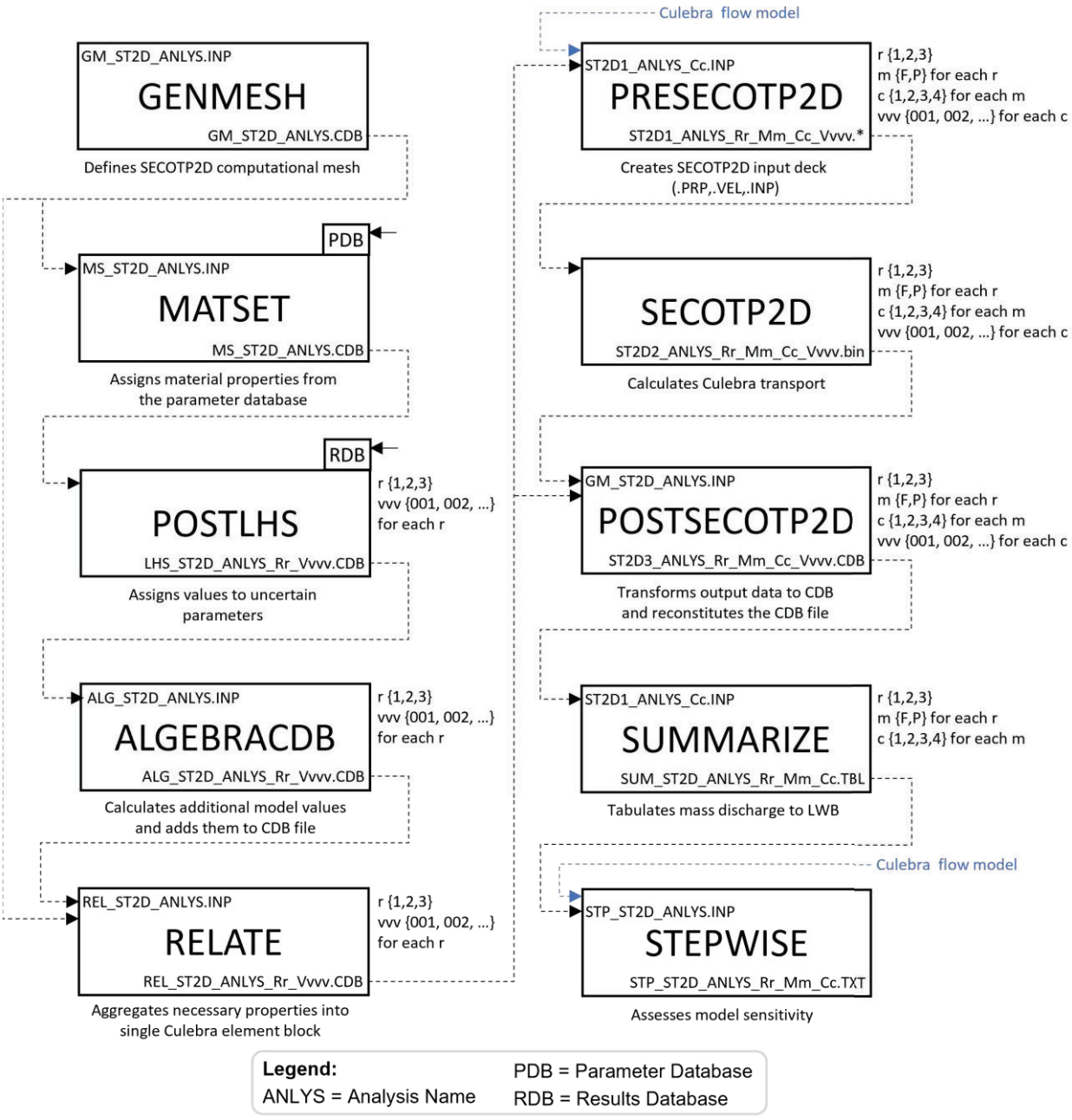

Figure 6. Culebra Transport Model Run Control Diagram

Information Only

5.0 RESULTS

This section presents results from the CRA-2026 flow, particle tracking, radionuclide mass transport, and sensitivity analysis calculations for full and partial mining scenarios, and compares results to the RPPCR. Results from all four CRPs are provided here which functionally encompasses both the interim and final state repositories. Figures show replicate 1 results, whereas tables report statistics for all three replicates. The only modification made in the CRA-2026 since the RPPCR that impacts results was a small change in the location of CRP 2 (see section 2.1). Accordingly, the only changes in the CRA-2026 results that occur relative to the RPPCR are those related to CRP 2. CRP 1, 3, and 4 are unchanged in the CRA-2026 relative to the RPPCR.

5.1 Flow

This section presents results from the CRA-2026 MODFLOW6 100-m flow simulations. Results are fetched from the MODFLOW 6 MODFLOW100m output flow files *Output/R{1,2,3}/{full,part}/v{vvv}/mf6_head.cbc*.

Figure 7 shows the ensemble average of $\log_{10}$ flow rates within the LWB for the CRA-2026 and RPPCR, for partial and full mining cases. No-mining flow rates are provided in Appendix 8. CRA-2026 used the same set of T-field as the RPPCR (see section 4.0, step 3). Furthermore, relative to the RPPCR there were no changes to Culebra flow fields (see section 4.0, step 4). Accordingly, CRA-2026 flow rates are identical to the RPPCR. As reported in the RPPCR a high-transmissivity pathway was observed during the SNL-14 pumping test (U.S. DOE 2014). The high-transmissivity pathway manifests as a linear north-south feature located in the southern half of the domain approximately following column 130. The edges of the areas affected by potash mining are visible in both mining scenarios, in the full mining case as an irregular shaped region with lighter color extending over the LWB everywhere but the southwest quadrant, and in the partial mining case just inside the periphery of the WIPP LWB.

The RPPCR showed the standard deviation of flow rates as well as flow direction. These are unchanged in the CRA-2026.

Information Only

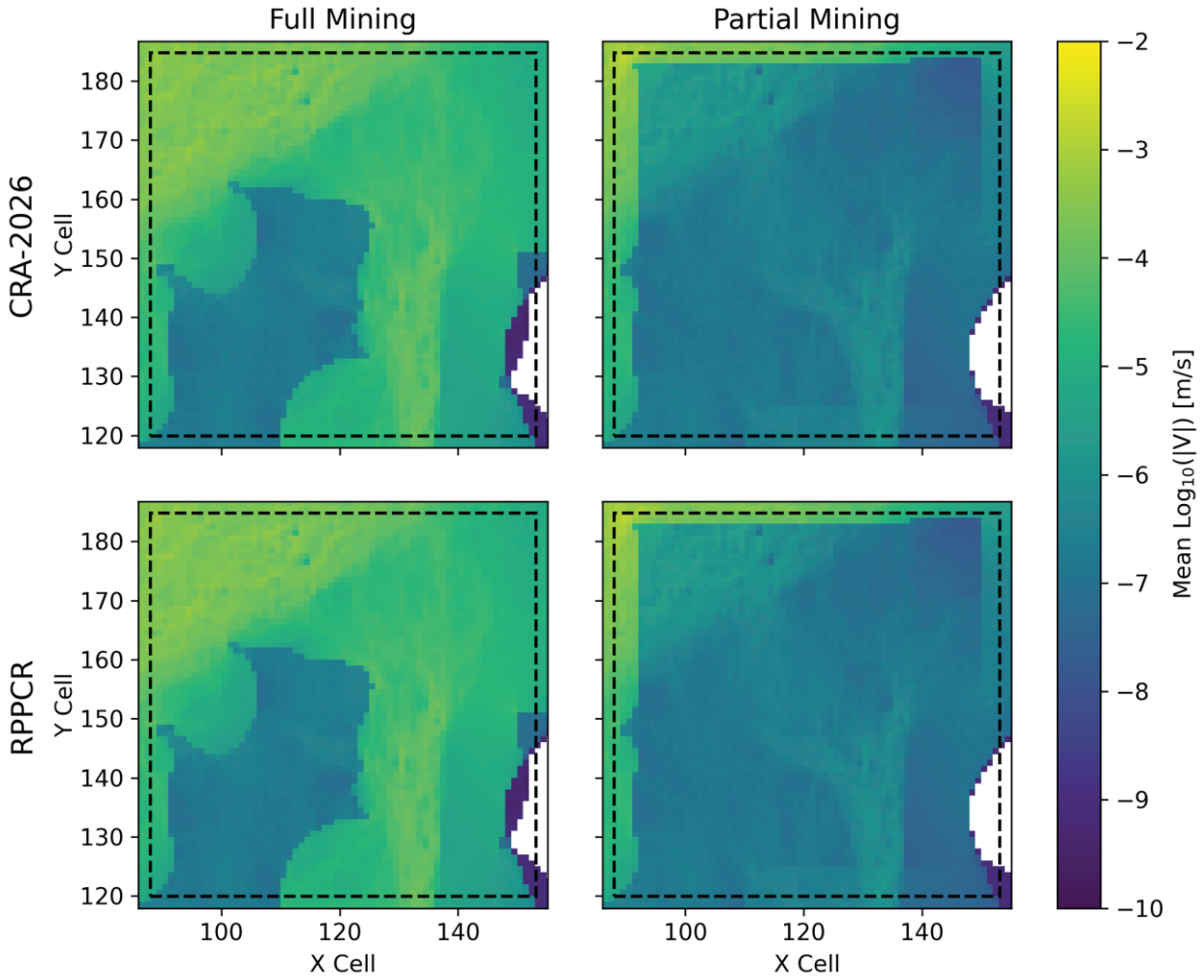

Figure 7. Ensemble Mean Flow Rate

5.2 Particle Tracking

This section presents results from the DTRKMF particle time and position output (*dtrk_mf6_CRA26_FS_r{1,2,3}_m{f,p}_c{1,2,3,4}_v{vvv}.out*), and the associated summary table files (*sum_mf6_CRA26_FS _r{1,2,3}_m{f,p}_c{1,2,3,4}_v{vvv}.tbl*).

Figure 8 compares particle travel time to the LWB for the CRA-2026 and the RPPCR. The gray dashed line is a 1:1 reference. Vectors with faster travel times to the LWB in the CRA-2026 plot below the reference. Rank correlations between analysis vectors and associated p-values were calculated with the Python stats package and are displayed directly on the figures. CRP 2 results indicate a strong correlation between the CRA-2026 and RPPCR for full (0.97) and partial (0.88) mining scenarios. The deviation away from 1:1 can be attributed to the change in location of CRP 2.

Information Only

Figure 9 shows map view spatial distribution of all 100 particle tracks with the mining-impacted area shown in gray. As in the RPPCR particle tracks from release points CRP 1, 2, and 3 show downstream flow generally oriented toward the south. In the full mining scenario, particle tracks show the flow field is typically oriented toward the full mining impacted area to the southeast, then deflects along the mining affected region interface to the southern LWB. The partial mining particle tracks are more broadly distributed across the east-west direction (i.e., not as focused by persistent features across realizations), but are also generally directed toward the south. In contrast, particle tracks from CRP 4 vary significantly between scenarios: the full mining particle tracks continue west then turn sharply to the south near the western edge of the LWB, while the partial mining particle tracks generally lead south. CRP 2 particle tracks from the CRA-2026 and RPPCR show slight initial differences near the release point, but differences diminish near the LWB.

Figure 10 shows cumulative distribution of the time taken for a particle to reach the LWB along each particle track, plotted as an exceedance probability. Conceptually, these plots describe the likelihood of a particle crossing the LWB within the range of observed particle travel times. As reported in the RPPCR particles exit the LWB in the full mining CRP 4 scenario significantly earlier than the other scenarios across all probability levels. Travel times to the LWB from the CRP 2 and CRP 3 release points are longer than travel times to the LWB from the CRP 1 release points. CRP 2 travel times to the LWB from the CRA-2026 are slightly shorter relative to the RPPCR at most probabilities.

Table 9 through Table 16 provide mean, median, minimum, and maximum particle travel times in years. As expected, all statistics are identical with exception of CRP 2. The slight differences in CRP 2 travel time to the LWB, and particle track paths results can be attributed to the location change of CRP 2 in the CRA-2026.

Information Only

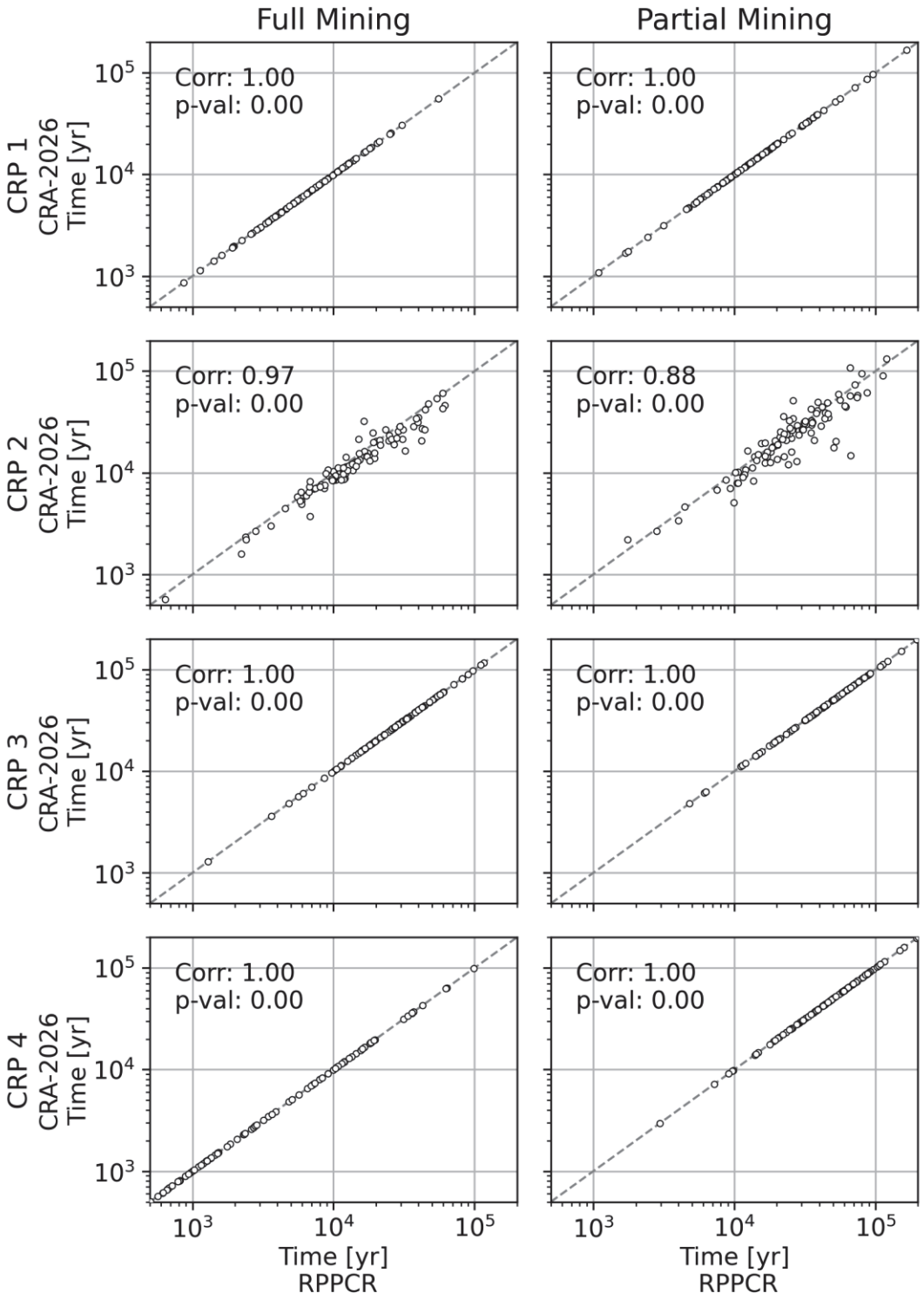

Figure 8. DTRKMF Particle Travel Time to LWB: CRA-2026 Versus RPPCR

Information Only

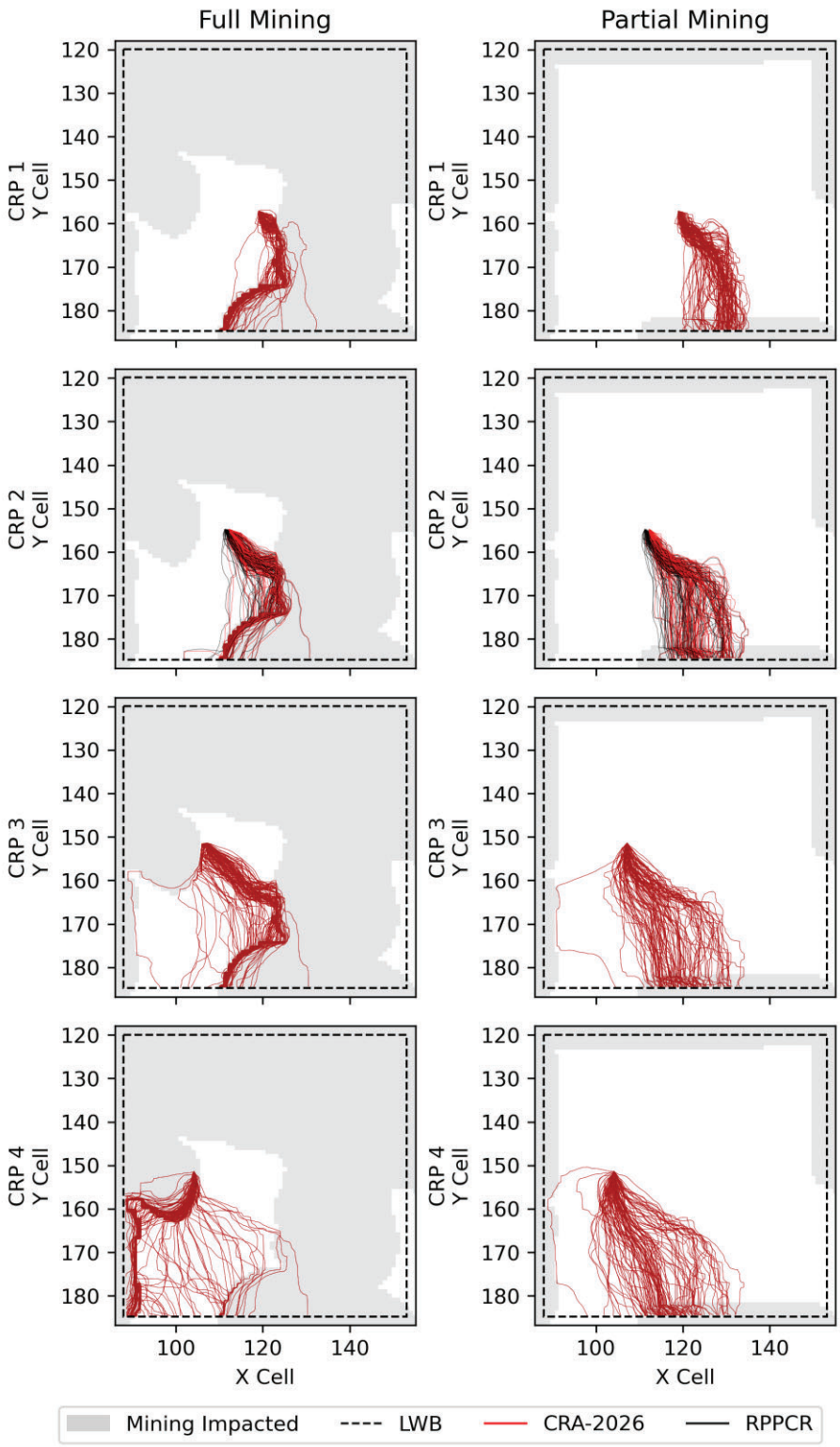

Figure 9. DTRKMF Particle Tracks

Information Only

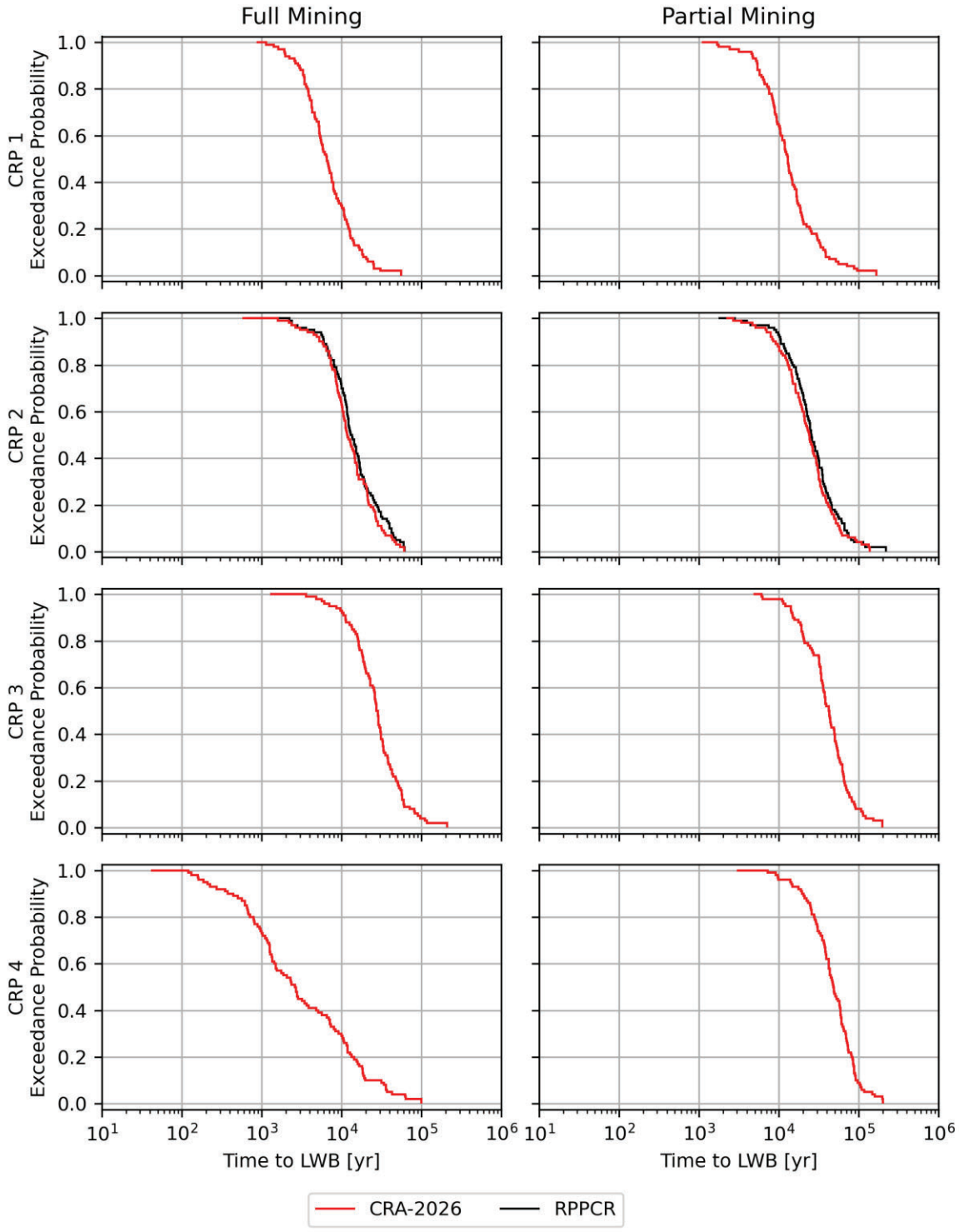

Figure 10. Particle Travel Time to LWB Exceedance Probabilities

Information Only

Table 9. Mean Particle Travel Time [yr] to LWB for Full Mining Scenario

	CRP1	CRP2	CRP3	CRP4
CRA-2026				
R1	8.57E+03	1.56E+04	3.40E+04	8.86E+03
R2	7.97E+03	1.57E+04	3.34E+04	9.35E+03
R3	8.38E+03	1.65E+04	3.43E+04	9.32E+03
RPPCR				
R1	8.57E+03	1.78E+04	3.40E+04	8.86E+03
R2	7.97E+03	1.79E+04	3.34E+04	9.35E+03
R3	8.38E+03	1.83E+04	3.43E+04	9.32E+03

Table 10. Median Particle Travel Time [yr] to LWB for Full Mining Scenario

	CRP1	CRP2	CRP3	CRP4
CRA-2026				
R1	6.49E+03	1.16E+04	2.72E+04	2.48E+03
R2	6.39E+03	1.28E+04	2.71E+04	1.91E+03
R3	6.23E+03	1.30E+04	2.80E+04	3.31E+03
RPPCR				
R1	6.49E+03	1.28E+04	2.72E+04	2.48E+03
R2	6.39E+03	1.35E+04	2.71E+04	1.91E+03
R3	6.23E+03	1.32E+04	2.80E+04	3.31E+03

Table 11. Minimum Particle Travel Time [yr] to LWB for Full Mining Scenario

	CRP1	CRP2	CRP3	CRP4
CRA-2026				
R1	8.66E+02	5.73E+02	1.29E+03	4.09E+01
R2	1.09E+03	6.30E+02	1.77E+03	3.99E+01
R3	9.23E+02	5.55E+02	1.41E+03	1.05E+02
RPPCR				
R1	8.66E+02	6.43E+02	1.29E+03	4.09E+01
R2	1.09E+03	7.49E+02	1.77E+03	3.99E+01
R3	9.23E+02	6.43E+02	1.41E+03	1.05E+02

Information Only

Table 12. Maximum Particle Travel Time [yr] to LWB for Full Mining Scenario

	CRP1	CRP2	CRP3	CRP4
CRA-2026				
R1	5.55E+04	6.08E+04	2.09E+05	9.90E+04
R2	2.91E+04	6.52E+04	2.03E+05	7.51E+04
R3	6.03E+04	8.12E+04	1.77E+05	5.61E+04
RPPCR				
R1	5.55E+04	6.15E+04	2.09E+05	9.90E+04
R2	2.91E+04	6.70E+04	2.03E+05	7.51E+04
R3	6.03E+04	8.95E+04	1.77E+05	5.61E+04

Table 13. Mean Particle Travel Time [yr] to LWB for Partial Mining Scenario

	CRP1	CRP2	CRP3	CRP4
CRA-2026				
R1	1.87E+04	2.96E+04	4.86E+04	5.53E+04
R2	1.70E+04	2.87E+04	5.06E+04	5.62E+04
R3	1.73E+04	2.85E+04	4.88E+04	5.43E+04
RPPCR				
R1	1.87E+04	3.32E+04	4.86E+04	5.53E+04
R2	1.70E+04	3.14E+04	5.06E+04	5.62E+04
R3	1.73E+04	3.05E+04	4.88E+04	5.43E+04

Table 14. Median Particle Travel Time [yr] to LWB for Partial Mining Scenario

	CRP1	CRP2	CRP3	CRP4
CRA-2026				
R1	1.29E+04	2.37E+04	4.22E+04	4.80E+04
R2	1.20E+04	2.39E+04	4.21E+04	4.75E+04
R3	1.21E+04	2.28E+04	4.31E+04	5.03E+04
RPPCR				
R1	1.29E+04	2.54E+04	4.22E+04	4.80E+04
R2	1.20E+04	2.79E+04	4.21E+04	4.75E+04
R3	1.21E+04	2.65E+04	4.31E+04	5.03E+04

Information Only

Table 15. Minimum Particle Travel Time [yr] to LWB for Partial Mining Scenario

	CRP1	CRP2	CRP3	CRP4
CRA-2026				
R1	1.09E+03	2.20E+03	4.79E+03	2.97E+03
R2	1.09E+03	2.20E+03	6.26E+03	4.70E+03
R3	5.70E+02	1.21E+03	2.83E+03	3.60E+03
RPPCR				
R1	1.09E+03	1.76E+03	4.79E+03	2.97E+03
R2	1.09E+03	1.76E+03	6.26E+03	4.70E+03
R3	5.70E+02	9.23E+02	2.83E+03	3.60E+03

Table 16. Maximum Particle Travel Time [yr] to LWB for Partial Mining Scenario

	CRP1	CRP2	CRP3	CRP4
CRA-2026				
R1	1.67E+05	1.37E+05	1.98E+05	2.02E+05
R2	9.12E+04	1.27E+05	2.45E+05	2.55E+05
R3	1.07E+05	1.00E+05	2.11E+05	1.38E+05
RPPCR				
R1	1.67E+05	2.17E+05	1.98E+05	2.02E+05
R2	9.12E+04	1.13E+05	2.45E+05	2.55E+05
R3	1.07E+05	1.09E+05	2.11E+05	1.38E+05

5.3 Radionuclide Transport

This section presents results from the SECOTP2D transport simulation summary output tables (*sum_st2d_CRA26_FS_r{1,2,3}_m{f,p}_c{1,2,3,4}.tbl*). Figures in this section report mass breakthrough and exceedance probability curves, while tables report cumulative release summary statistics for each radionuclide (^{241}Am, ^{239}Pu, ^{230}Th, ^{234}U, and ^{23A}Th).

Figure 11 and Figure 12 compare mass breakthrough at 10,000 years for the CRA-2026 and RPPCR. The gray dashed line is a 1:1 reference. Vectors with larger mass breakthrough at 10,000 years in the CRA-2026 plot above the reference. Results are shown on logarithmic axes. The 10^{-9} kg significance threshold was chosen for consistency with the PABC-2004 and PABC09 report (Lowry and Kanney 2005; Kuhlman 2010). CRP 2 results show clustering around, and slightly above, the 1:1 reference indicating vectors with mass breakthrough > 10^{-9} kg at 10,000 years are bias toward slight increases in the CRA-2026 relative to the RPPCR.

Information Only

Figure 13 and Figure 14 show breakthrough curves of mass discharge to the LWB over time. The breakthrough curves are shown on a linear ordinate from 0 to 1 kg. All 100 simulations are included in each subplot, though in many subplots vectors plot very close to the x-axis over the entire simulation period. Except for a few simulations of the CRP 2 scenario, CRA-2026 and RPPCR results coincide. In general, mass discharge breakthrough curves show earlier, more complete, and more frequent breakthrough in the full mining scenario than the partial mining scenario for all radionuclides and release points, particularly for CRP 4. The most prominent curves in the partial mining scenario are from ^{234}U. Furthermore, ^{234}U is the only radionuclide with breakthrough curves (CRP 2) that are discernably different between the CRA-2026 and RPPCR. However, visible differences in mean breakthrough curves between the CRA-2026 and RPPCR are not apparent.

Figure 15 through Figure 19 show exceedance probability curves of cumulative mass reaching the LWB by 10,000 years. Except for a few simulations of the CRP 2 scenario, CRA-2026 and RPPCR curves coincide. Consistent with Figure 11 and Figure 12 mass discharge is shown on a logarithmic scale on the x-axis from 10^{-9} to 1 kg. Some partial mining scenario subplots display no results due to the low predictions of mass to the LWB. The exceedance probability curves also demonstrate that the cumulative releases at 10,000 years are higher in the full mining scenario than in the partial mining scenario for all radionuclides across all displayed probability ranges. The differences are most apparent in CRP 4 where full mining scenario results are significantly larger than partial mining results. In the full mining scenario, CRP 2 and CRP 3 releases are generally lower than CRP 1, which in turn are lower than CRP 4, for all radionuclides. The CRA-2026 CRP 2 results are similar to slightly increased relative to the RPPCR, consistent with mass breakthrough results.

Table 17 through Table 46 provide summary statistics of cumulative mass transported to the LWB over 10,000 years (released) including the mean, median, and maximum. Values below 10^{-24} kg are tabulated as zero. Table 17 through Table 22 report statistics for ^{241}Am, Table 23 through Table 28 report statistics for ^{239}Pu, Table 29 through Table 34 report statistics for ^{23A}Th, Table 35 through Table 40 report statistics for ^{234}U, and Table 41 through Table 46 report statistics for ^{230}Th. As in the RPPCR, cumulative mass transported to the LWB from ^{241}Am are typically lowest and ^{234}U are the highest, with the ^{23A}Th and ^{239}Pu values in-between, for all release points and mining scenarios.

Under full mining conditions, the mean cumulative mass transported is highest for all radionuclides in CRP 4 simulations (Table 17, Table 23, Table 29, Table 35, and Table 41). Under partial mining conditions, mean cumulative mass transported to the LWB is typically highest in CRP 4 for ^{241}Am and in CRP 1 for ^{239}Pu, ^{23A}Th, ^{234}U, and ^{230}Th (Table 20, Table 26, Table 32, Table 38, and Table 44). Examining mean cumulative mass transported from CRP 2 reveals small quantitative differences between CRA-2026 and RPPCR. These differences are imperceptible in mean breakthrough curves of mass discharge but are consistent with mass breakthrough scatterplots of CRP 2 revealing a bias toward slight increases in the CRA-2026 relative to the RPPCR.

Information Only

Median cumulative mass transported is similar to mean mass transported, where mass transported is highest for all radionuclides in the full mining CRP 4 simulations (Table 18, Table 24, Table 30, Table 36, and Table 42). However, mass values are orders of magnitude lower than in their mean counterparts. Partial mining scenario median mass values are below the reporting criterion of 10^{-24} kg for all radionuclides (Table 21, Table 27, Table 33, Table 39, Table 45). For CRP 2, values of median cumulative mass transported for the CRA-2026 and the RPPCR are also below the reporting threshold.

Tables of maximum mass transported show that ^{234}U has near complete breakthrough from all release points in the full mining scenario (Table 19, Table 25, Table 31, Table 37, and Table 43). Due to acceptable mass balance limits, maximum cumulative mass can slightly exceed 1.00 kg (WIPP PA 2022). In partial mining scenarios ^{234}U shows highest maximum mass breakthrough amongst radionuclides consistent with Figure 14. For radionuclides other than ^{234}U, full mining CRP 4 simulations result in the highest maximum mass breakthrough. This is also true for the partial mining scenario in replicate 1, but highest maximum values from replicate 2 and 3 results are more mixed amongst CRPs (Table 22, Table 28, Table 34, Table 40, and Table 46). For CRP 2, maximum cumulative mass transported values in the CRA-2026 are similar to slightly higher relative to the RPPCR.

Table 47 through Table 56 provide number of vectors (counts) with greater than $> 10^{-9}$ kg cumulative mass transported to the LWB over 10,000 years. Table 47 and Table 48 report counts for ^{241}Am, Table 49 and Table 50 report counts for ^{239}Pu, Table 51 and Table 52 report counts for ^{234}U, Table 53 and Table 54 report counts for ^{23A}Th, and Table 55 and Table 56 report statistics for ^{230}Th. The results show greater numbers of vectors exceeding the threshold for all radionuclides in the full mining CRP 4 scenario than in the other scenarios (Table 47, Table 49, Table 51, Table 53, and Table 55). In the partial mining scenario, the greatest number of vectors exceeding the threshold occurred in CRP 1 for all radionuclides, except for ^{241}Am, which had the most exceedances in CRP 4 simulations, though relatively few are observed across all scenarios (Table 48, Table 50, Table 52, Table 54, and Table 56). For CRP 2 full and partial mining scenarios, CRA-2026 counts either match RPPCR counts or exceed them by a few vectors.

Information Only

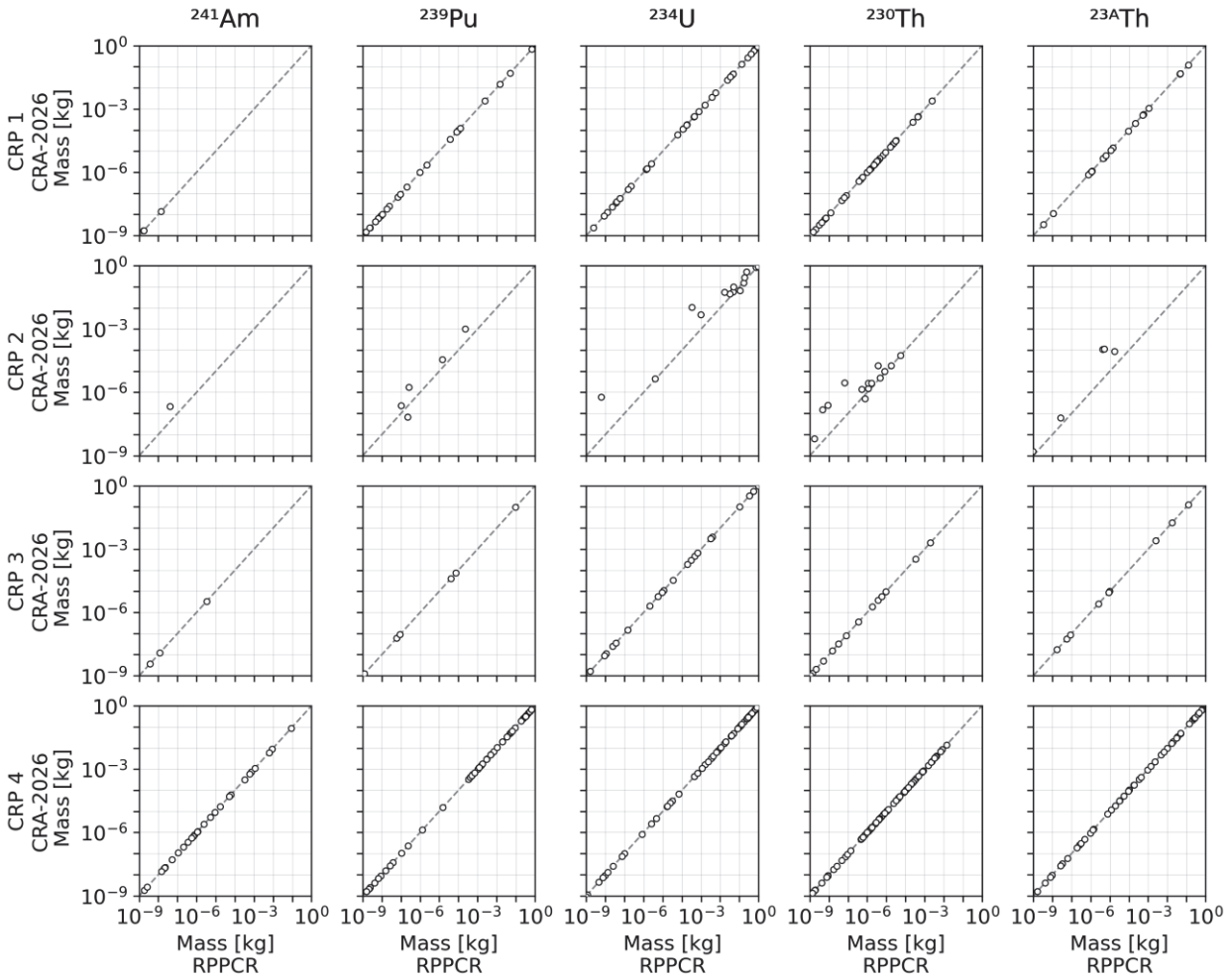

Figure 11. Mass Breakthrough at 10,000-yr: CRA-2026 Versus RPPCR Full Mining Scenario

Information Only

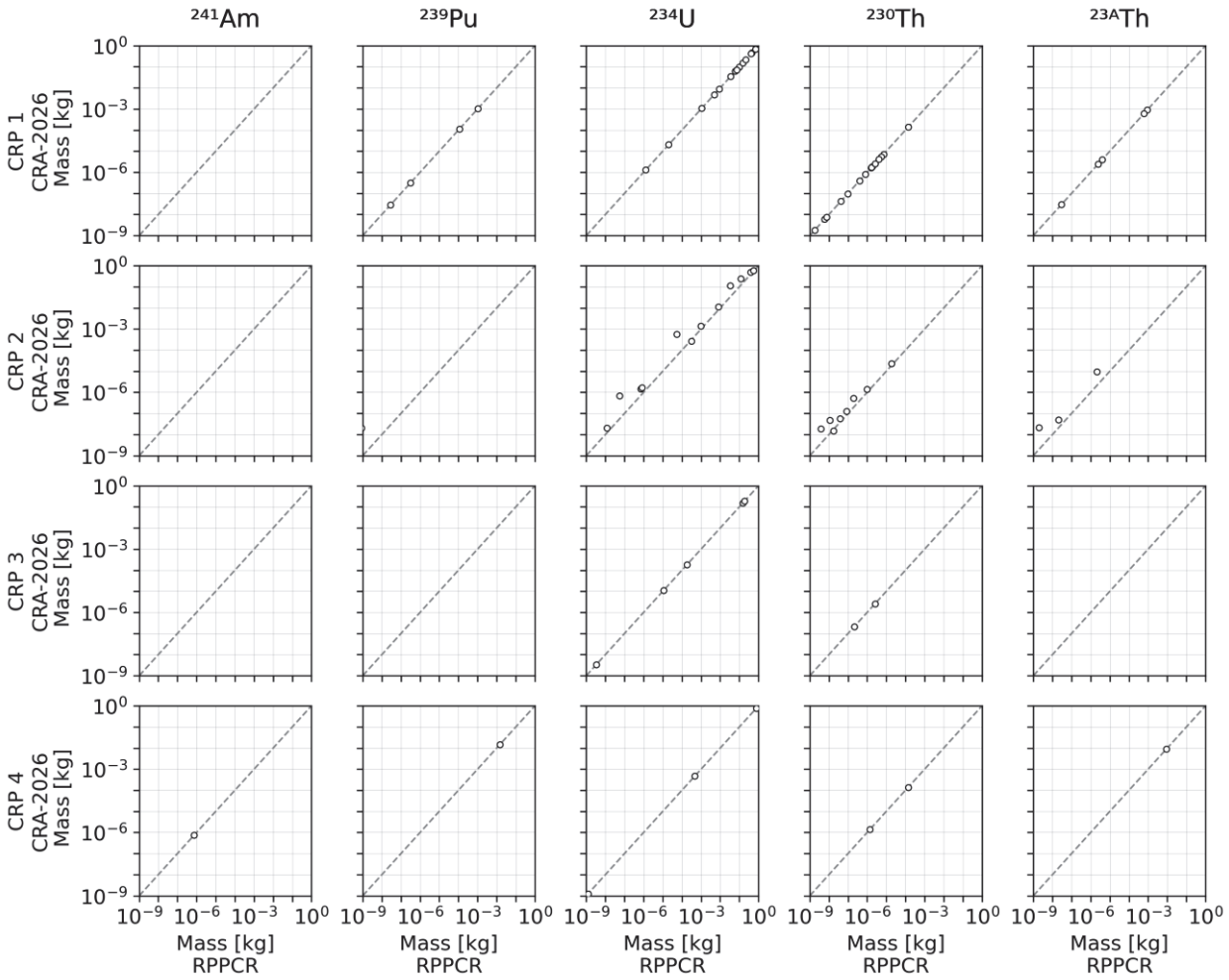

Figure 12. Mass Breakthrough at 10,000-yr: CRA-2026 Versus RPPCR Partial Mining Scenario

Information Only

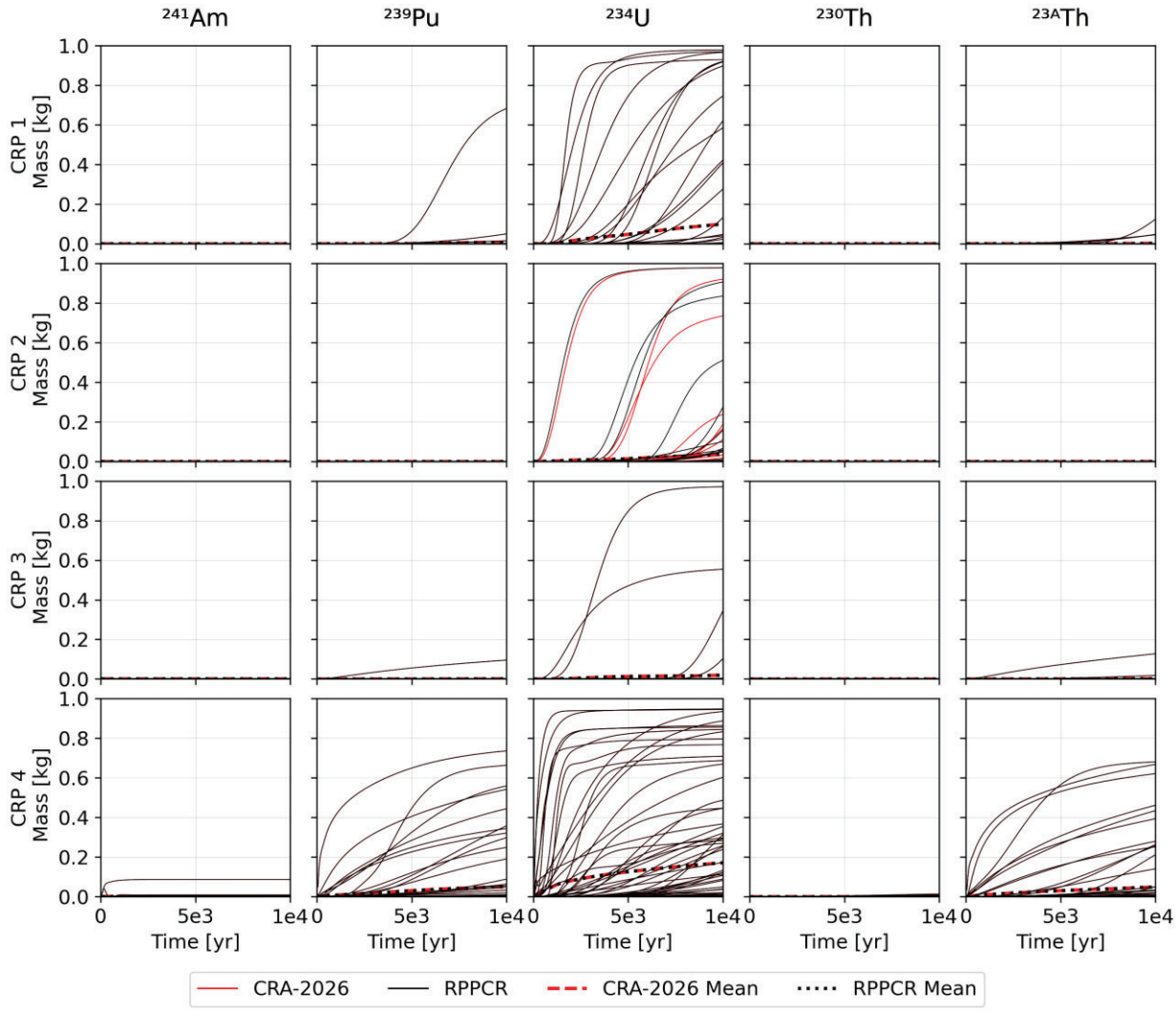

Figure 13. Mass Breakthrough Over Time: CRA-2026 Versus RPPCR Full Mining Scenario

Information Only

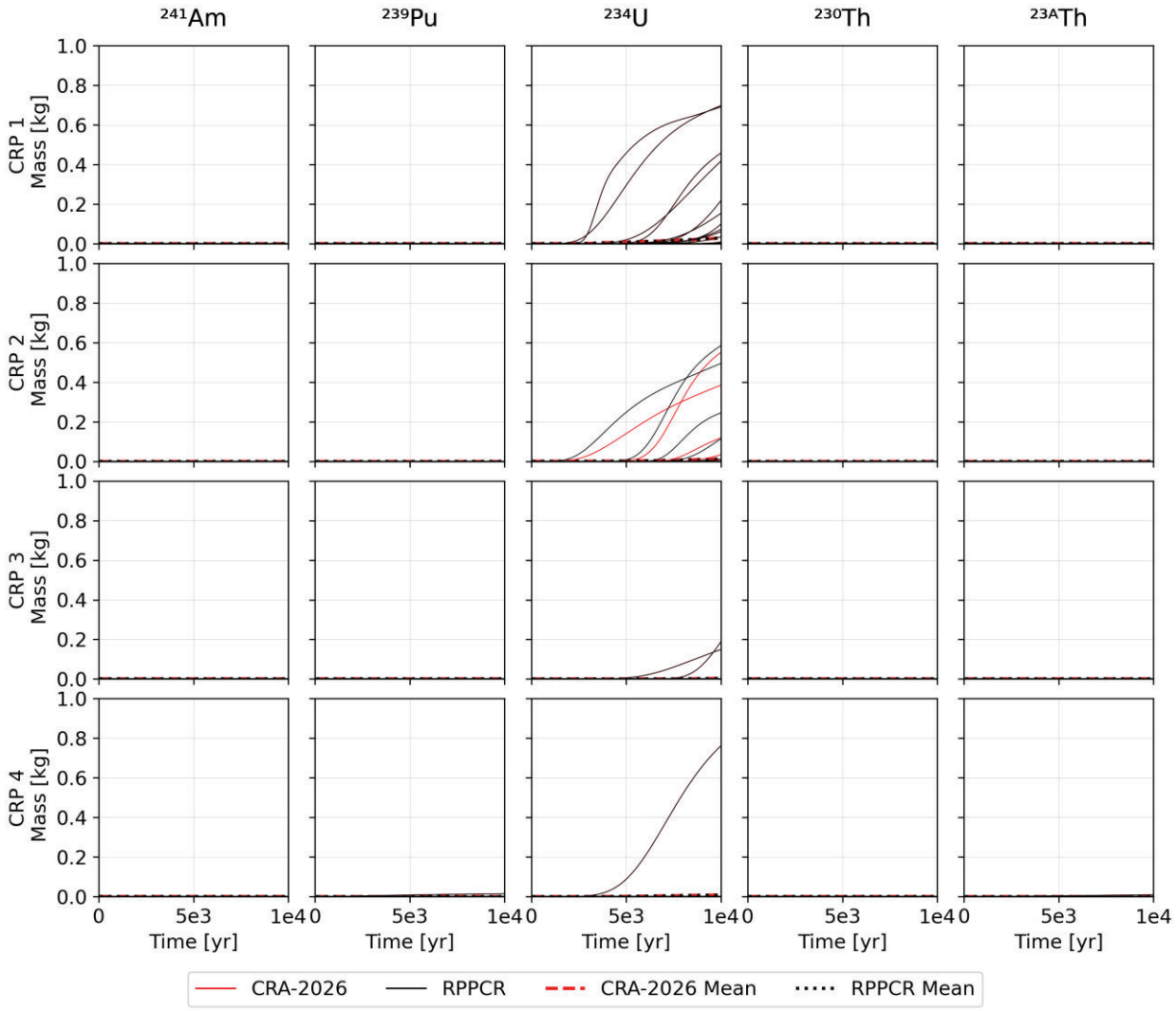

Figure 14. Mass Breakthrough Over Time: CRA-2026 Versus RPPCR Partial Mining Scenario

Information Only

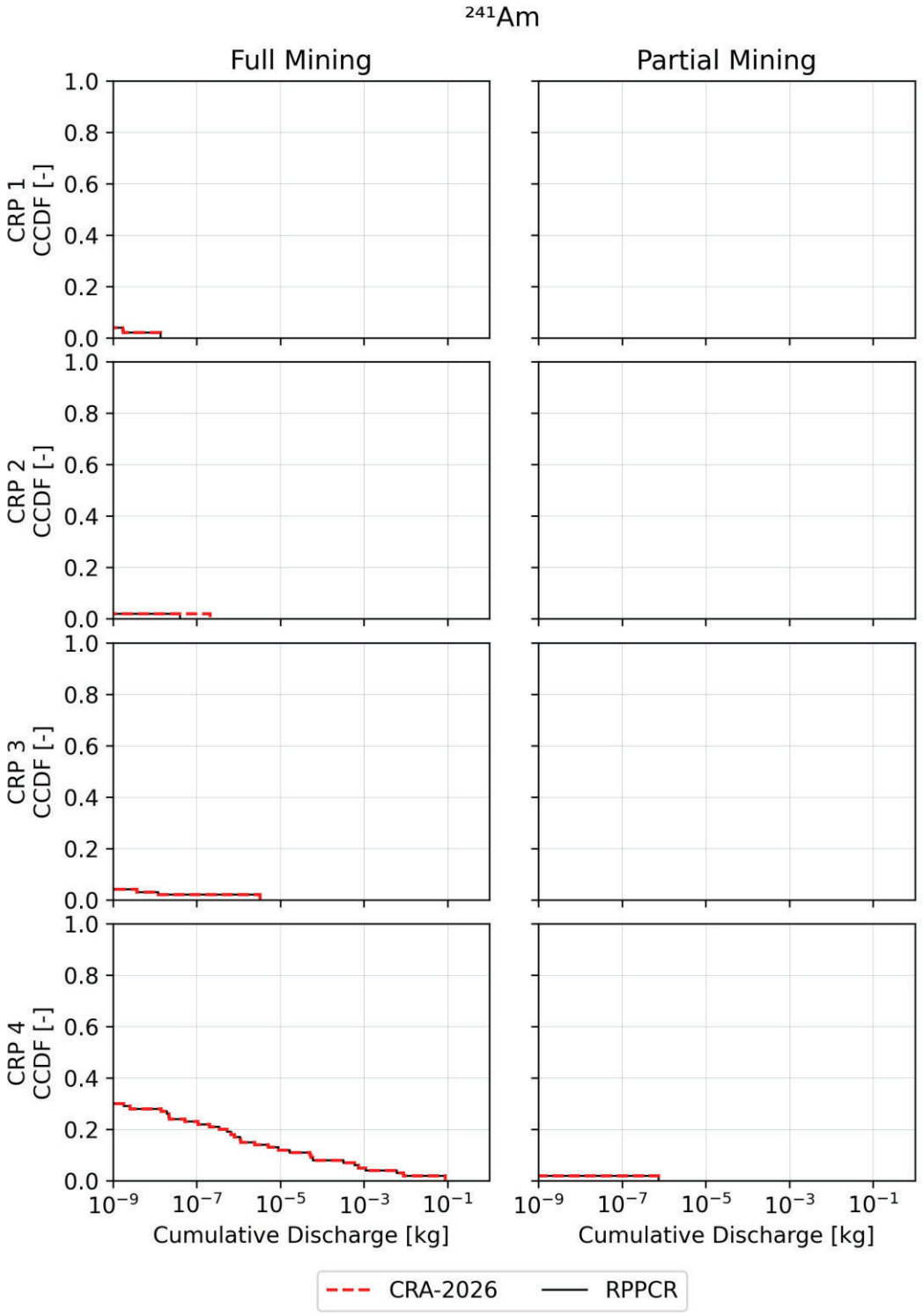

Figure 15. Exceedance Probability of ^{241}Am Mass to LWB in 10,000 Years

Information Only

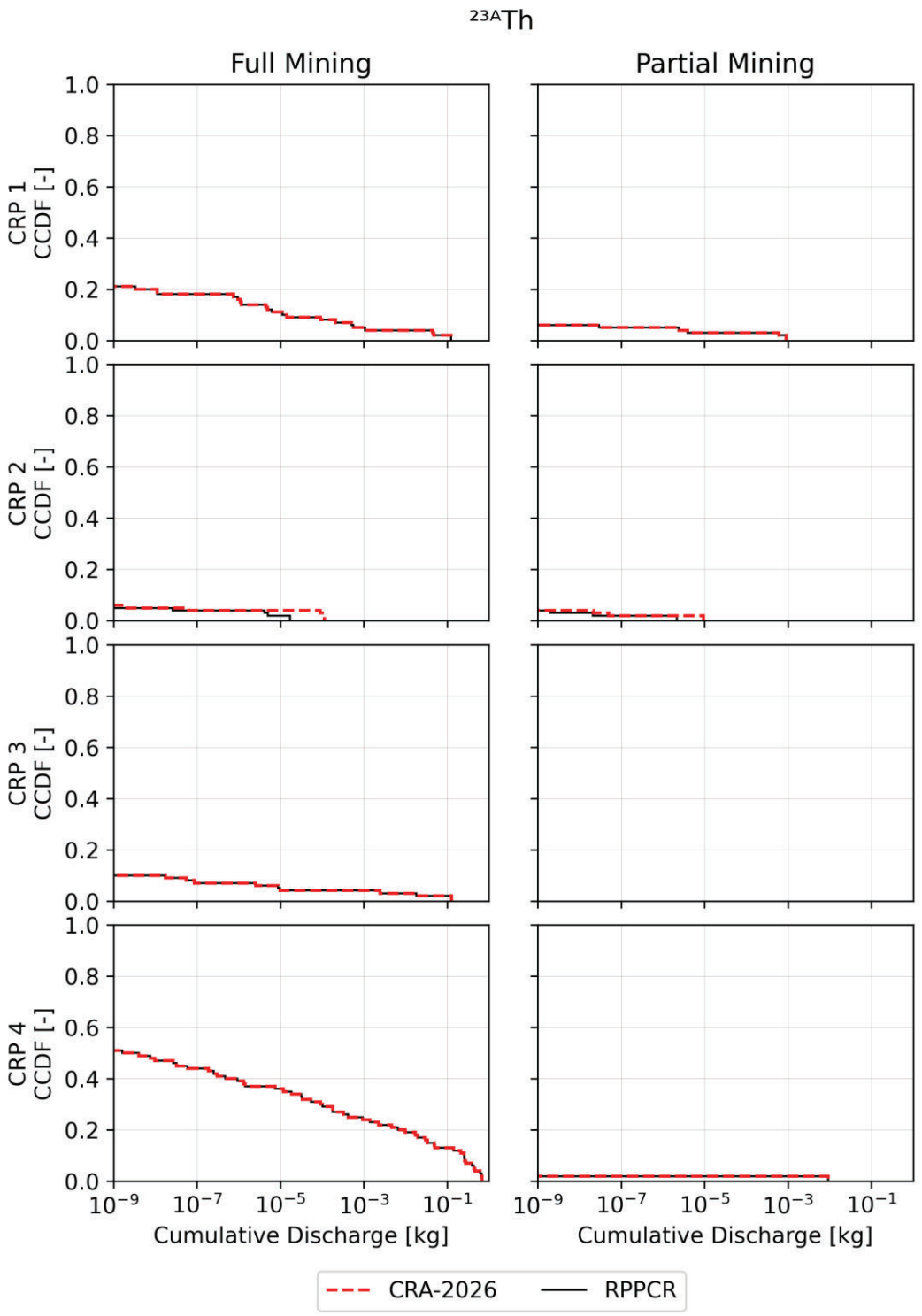

Figure 16. Exceedance Probability of ^{23A}Th Mass to LWB in 10,000 Years

Information Only

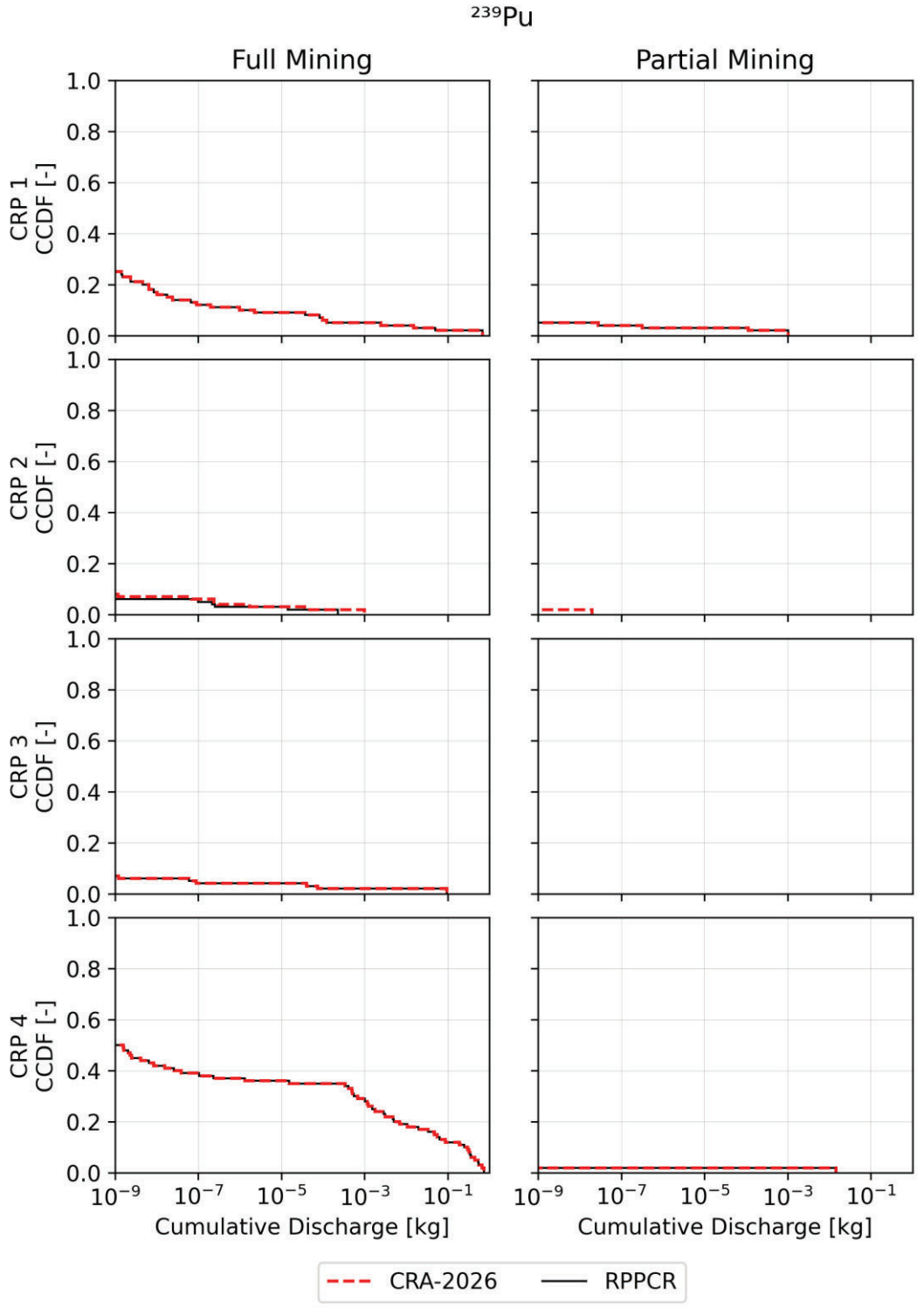

Figure 17. Exceedance Probability of ^{239}Pu Mass to the LWB in 10,000 Years

Information Only

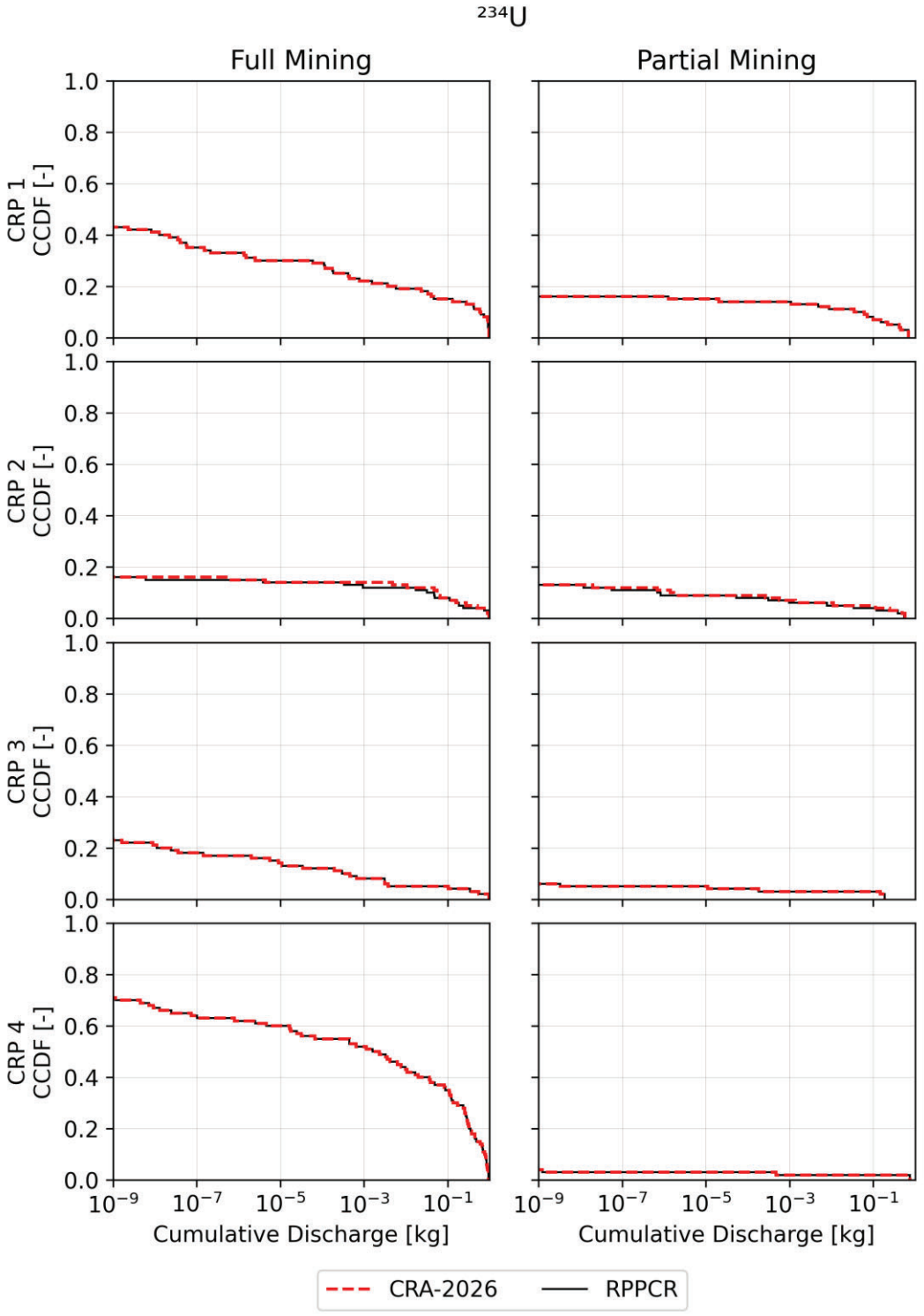

Figure 18. Exceedance Probability of ^{234}U Mass to LWB in 10,000 Years

Information Only

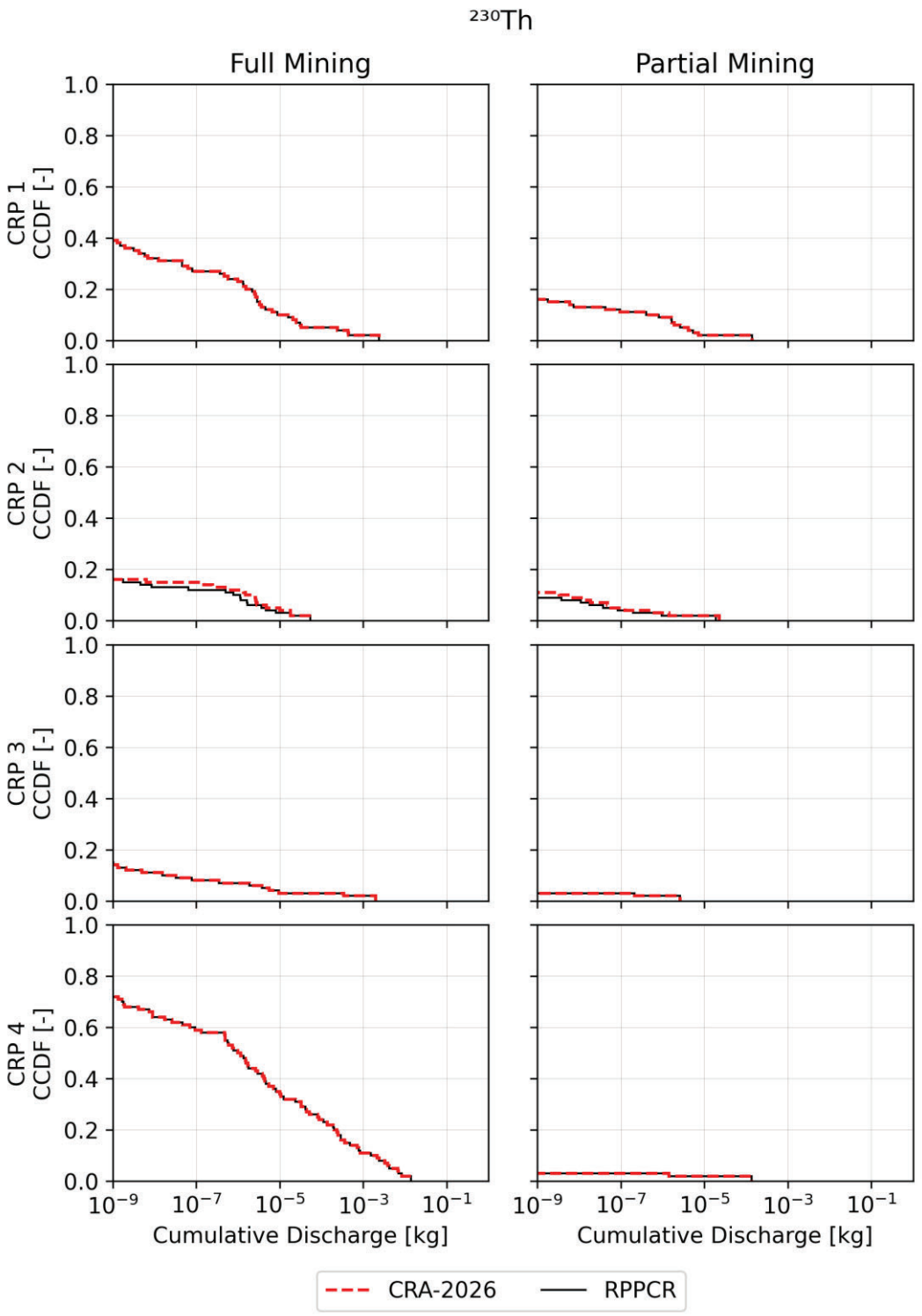

Figure 19. Exceedance Probability of ^{230}Th Mass to LWB in 10,000 Years

Information Only

Table 17. Mean Cumulative Mass [kg] of ^{241}Am to LWB for Full Mining Scenario

	CRP 1	CRP 2	CRP 3	CRP 4
CRA-2026				
R1	1.40E-10	2.12E-09	3.33E-08	1.05E-03
R2	1.07E-10	2.34E-12	2.66E-06	3.78E-03
R3	1.74E-10	1.25E-12	2.37E-08	9.60E-04
RPPCR				
R1	1.40E-10	4.02E-10	3.33E-08	1.05E-03
R2	1.07E-10	1.74E-12	2.66E-06	3.78E-03
R3	1.74E-10	1.02E-13	2.37E-08	9.60E-04

Table 18. Median Cumulative Mass [kg] of ^{241}Am to LWB for Full Mining Scenario

	CRP 1	CRP 2	CRP 3	CRP 4
CRA-2026				
R1	1.29E-24	0.00E+00	0.00E+00	7.66E-17
R2	6.51E-23	0.00E+00	0.00E+00	5.18E-16
R3	4.41E-23	0.00E+00	0.00E+00	8.42E-16
RPPCR				
R1	1.29E-24	0.00E+00	0.00E+00	7.66E-17
R2	6.51E-23	0.00E+00	0.00E+00	5.18E-16
R3	4.41E-23	0.00E+00	0.00E+00	8.42E-16

Table 19. Maximum cumulative mass [kg] of ^{241}Am to LWB for Full Mining Scenario

	CRP 1	CRP 2	CRP 3	CRP 4
CRA-2026				
R1	1.39E-08	2.12E-07	3.31E-06	8.71E-02
R2	8.04E-09	2.67E-10	2.66E-04	2.43E-01
R3	2.29E-08	1.19E-10	2.37E-06	6.74E-02
RPPCR				
R1	1.39E-08	4.02E-08	3.31E-06	8.71E-02
R2	8.04E-09	1.57E-10	2.66E-04	2.43E-01
R3	2.29E-08	8.43E-12	2.37E-06	6.74E-02

Information Only

Table 20. Mean Cumulative Mass [kg] of ^{241}Am to LWB for Partial Mining Scenario

	CRP 1	CRP 2	CRP 3	CRP 4
CRA-2026				
R1	1.78E-23	2.61E-21	5.42E-22	7.43E-09
R2	3.99E-21	2.10E-23	7.21E-18	2.72E-08
R3	0.00E+00	0.00E+00	1.04E-23	1.52E-15
RPPCR				
R1	1.78E-23	1.27E-22	5.42E-22	7.43E-09
R2	3.99E-21	0.00E+00	7.21E-18	2.72E-08
R3	0.00E+00	0.00E+00	1.04E-23	1.52E-15

Table 21. Median Cumulative Mass [kg] of ^{241}Am to LWB for Partial Mining Scenario

	CRP 1	CRP 2	CRP 3	CRP 4
CRA-2026				
R1	0.00E+00	0.00E+00	0.00E+00	0.00E+00
R2	0.00E+00	0.00E+00	0.00E+00	0.00E+00
R3	0.00E+00	0.00E+00	0.00E+00	0.00E+00
RPPCR				
R1	0.00E+00	0.00E+00	0.00E+00	0.00E+00
R2	0.00E+00	0.00E+00	0.00E+00	0.00E+00
R3	0.00E+00	0.00E+00	0.00E+00	0.00E+00

Table 22. Maximum Cumulative Mass [kg] of ^{241}Am to LWB for Partial Mining Scenario

	CRP 1	CRP 2	CRP 3	CRP 4
CRA-2026				
R1	1.78E-21	2.61E-19	3.67E-20	7.43E-07
R2	3.99E-19	2.10E-21	7.07E-16	2.72E-06
R3	0.00E+00	0.00E+00	4.59E-22	1.52E-13
RPPCR				
R1	1.78E-21	1.27E-20	3.67E-20	7.43E-07
R2	3.99E-19	3.70E-23	7.07E-16	2.72E-06
R3	0.00E+00	0.00E+00	4.59E-22	1.52E-13

Information Only

Table 23. Mean Cumulative Mass [kg] of ^{239}Pu to LWB for Full Mining Scenario

	CRP 1	CRP 2	CRP 3	CRP 4
CRA-2026				
R1	7.51E-03	1.03E-05	9.57E-04	5.06E-02
R2	1.11E-04	5.86E-05	5.54E-06	3.45E-02
R3	7.71E-03	9.26E-03	5.53E-05	5.89E-02
RPPCR				
R1	7.51E-03	2.44E-06	9.57E-04	5.06E-02
R2	1.11E-04	8.44E-06	5.54E-06	3.45E-02
R3	7.71E-03	8.19E-03	5.53E-05	5.89E-02

Table 24. Median Cumulative Mass [kg] of ^{239}Pu to LWB for Full Mining Scenario

	CRP 1	CRP 2	CRP 3	CRP 4
CRA-2026				
R1	2.59E-18	0.00E+00	0.00E+00	4.82E-10
R2	6.85E-18	0.00E+00	0.00E+00	1.36E-07
R3	2.36E-18	0.00E+00	0.00E+00	2.47E-11
RPPCR				
R1	2.59E-18	0.00E+00	0.00E+00	4.82E-10
R2	6.85E-18	0.00E+00	0.00E+00	1.36E-07
R3	2.36E-18	0.00E+00	0.00E+00	2.47E-11

Table 25. Maximum Cumulative Mass [kg] of ^{239}Pu to LWB for Full Mining Scenario

	CRP 1	CRP 2	CRP 3	CRP 4
CRA-2026				
R1	6.83E-01	9.95E-04	9.56E-02	7.36E-01
R2	6.53E-03	4.77E-03	4.36E-04	6.41E-01
R3	6.72E-01	8.08E-01	2.35E-03	7.19E-01
RPPCR				
R1	6.83E-01	2.29E-04	9.56E-02	7.36E-01
R2	6.53E-03	6.58E-04	4.36E-04	6.41E-01
R3	6.72E-01	7.34E-01	2.35E-03	7.19E-01

Information Only

Table 26. Mean Cumulative Mass [kg] of ^{239}Pu to LWB for Partial Mining Scenario

	CRP 1	CRP 2	CRP 3	CRP 4
CRA-2026				
R1	1.15E-05	1.99E-10	4.79E-20	1.46E-04
R2	6.89E-08	8.51E-09	1.65E-15	1.05E-10
R3	8.00E-03	5.24E-03	4.24E-05	3.02E-09
RPPCR				
R1	1.15E-05	8.49E-12	4.79E-20	1.46E-04
R2	6.89E-08	2.46E-09	1.65E-15	1.05E-10
R3	8.00E-03	5.77E-03	4.24E-05	3.02E-09

Table 27. Median Cumulative Mass [kg] of ^{239}Pu to LWB for Partial Mining Scenario

	CRP 1	CRP 2	CRP 3	CRP 4
CRA-2026				
R1	0.00E+00	0.00E+00	0.00E+00	0.00E+00
R2	0.00E+00	0.00E+00	0.00E+00	0.00E+00
R3	0.00E+00	0.00E+00	0.00E+00	0.00E+00
RPPCR				
R1	0.00E+00	0.00E+00	0.00E+00	0.00E+00
R2	0.00E+00	0.00E+00	0.00E+00	0.00E+00
R3	0.00E+00	0.00E+00	0.00E+00	0.00E+00

Table 28. Maximum Cumulative Mass [kg] of ^{239}Pu to LWB for Partial Mining Scenario

	CRP 1	CRP 2	CRP 3	CRP 4
CRA-2026				
R1	1.04E-03	1.99E-08	2.84E-18	1.46E-02
R2	6.88E-06	8.46E-07	9.20E-16	1.05E-08
R3	8.00E-01	5.24E-01	4.24E-03	2.27E-07
RPPCR				
R1	1.04E-03	8.49E-10	2.84E-18	1.46E-02
R2	6.88E-06	2.45E-07	9.20E-16	1.05E-08
R3	8.00E-01	5.77E-01	4.24E-03	2.27E-07

Information Only

Table 29. Mean Cumulative Mass [kg] of ^{23A}Th to LWB for Full Mining Scenario

	CRP 1	CRP 2	CRP 3	CRP 4
CRA-2026				
R1	2.19E-03	3.13E-06	1.48E-03	4.89E-02
R2	6.17E-03	6.19E-04	3.05E-05	4.46E-02
R3	1.11E-03	1.87E-03	1.44E-05	5.38E-02
RPPCR				
R1	2.19E-03	2.63E-07	1.48E-03	4.89E-02
R2	6.17E-03	3.25E-04	3.05E-05	4.46E-02
R3	1.11E-03	1.24E-03	1.44E-05	5.38E-02

Table 30. Median Cumulative Mass [kg] of ^{23A}Th to LWB for Full Mining Scenario

	CRP 1	CRP 2	CRP 3	CRP 4
CRA-2026				
R1	7.69E-18	0.00E+00	0.00E+00	1.17E-09
R2	3.87E-18	0.00E+00	0.00E+00	2.28E-09
R3	2.02E-19	0.00E+00	0.00E+00	2.74E-09
RPPCR				
R1	7.69E-18	0.00E+00	0.00E+00	1.17E-09
R2	3.87E-18	0.00E+00	0.00E+00	2.28E-09
R3	2.02E-19	0.00E+00	0.00E+00	2.74E-09

Table 31. Maximum Cumulative Mass [kg] of ^{23A}Th to LWB for Full Mining Scenario

	CRP 1	CRP 2	CRP 3	CRP 4
CRA-2026				
R1	1.24E-01	1.14E-04	1.28E-01	6.81E-01
R2	5.72E-01	6.19E-02	2.58E-03	7.13E-01
R3	4.22E-02	9.42E-02	1.04E-03	8.69E-01
RPPCR				
R1	1.24E-01	1.71E-05	1.28E-01	6.81E-01
R2	5.72E-01	3.25E-02	2.58E-03	7.13E-01
R3	4.22E-02	6.52E-02	1.04E-03	8.69E-01

Information Only

Table 32. Mean Cumulative Mass [kg] of ^{23A}Th to LWB for Partial Mining Scenario

	CRP 1	CRP 2	CRP 3	CRP 4
CRA-2026				
R1	1.50E-05	9.39E-08	6.66E-19	9.16E-05
R2	2.89E-05	3.24E-10	7.40E-15	7.67E-11
R3	8.71E-05	9.33E-06	5.67E-11	5.30E-07
RPPCR				
R1	1.50E-05	2.17E-08	6.66E-19	9.16E-05
R2	2.89E-05	4.10E-11	7.40E-15	7.67E-11
R3	8.71E-05	2.74E-06	5.67E-11	5.30E-07

Table 33. Median Cumulative Mass [kg] of ^{23A}Th to LWB for Partial Mining Scenario

	CRP 1	CRP 2	CRP 3	CRP 4
CRA-2026				
R1	0.00E+00	0.00E+00	0.00E+00	0.00E+00
R2	0.00E+00	0.00E+00	0.00E+00	0.00E+00
R3	0.00E+00	0.00E+00	0.00E+00	0.00E+00
RPPCR				
R1	0.00E+00	0.00E+00	0.00E+00	0.00E+00
R2	0.00E+00	0.00E+00	0.00E+00	0.00E+00
R3	0.00E+00	0.00E+00	0.00E+00	0.00E+00

Table 34. Maximum Cumulative Mass [kg] of ^{23A}Th to LWB for Partial Mining Scenario

	CRP 1	CRP 2	CRP 3	CRP 4
CRA-2026				
R1	8.94E-04	9.32E-06	6.56E-17	9.16E-03
R2	2.80E-03	2.83E-08	7.45E-13	4.62E-13
R3	8.70E-03	9.09E-04	5.67E-09	5.29E-05
RPPCR				
R1	8.94E-04	2.15E-06	6.56E-17	9.16E-03
R2	2.80E-03	4.08E-09	7.45E-13	4.62E-13
R3	8.70E-03	2.69E-04	5.67E-09	5.29E-05

Information Only

Table 35. Mean Cumulative Mass [kg] of ^{234}U to LWB for Full Mining Scenario

	CRP 1	CRP 2	CRP 3	CRP 4
CRA-2026				
R1	9.93E-02	4.00E-02	1.98E-02	1.71E-01
R2	8.32E-02	3.31E-02	1.27E-02	1.81E-01
R3	1.10E-01	4.21E-02	1.83E-02	1.80E-01
RPPCR				
R1	9.93E-02	3.48E-02	1.98E-02	1.71E-01
R2	8.32E-02	2.94E-02	1.27E-02	1.81E-01
R3	1.10E-01	3.78E-02	1.83E-02	1.80E-01

Table 36. Median Cumulative Mass [kg] of ^{234}U to LWB for Full Mining Scenario

	CRP 1	CRP 2	CRP 3	CRP 4
CRA-2026				
R1	1.18E-11	0.00E+00	2.76E-24	1.37E-03
R2	2.84E-12	0.00E+00	4.96E-23	1.29E-03
R3	3.99E-12	0.00E+00	1.86E-23	2.93E-04
RPPCR				
R1	1.18E-11	0.00E+00	2.76E-24	1.37E-03
R2	2.84E-12	0.00E+00	4.96E-23	1.29E-03
R3	3.99E-12	0.00E+00	1.86E-23	2.93E-04

Table 37. Maximum Cumulative Mass [kg] of ^{234}U to LWB for Full Mining Scenario

	CRP 1	CRP 2	CRP 3	CRP 4
CRA-2026				
R1	9.79E-01	9.78E-01	9.71E-01	9.48E-01
R2	9.91E-01	8.63E-01	5.23E-01	9.26E-01
R3	9.74E-01	9.45E-01	9.24E-01	9.46E-01
RPPCR				
R1	9.79E-01	9.77E-01	9.71E-01	9.48E-01
R2	9.91E-01	8.51E-01	5.23E-01	9.26E-01
R3	9.74E-01	9.46E-01	9.24E-01	9.46E-01

Information Only

Table 38. Mean Cumulative Mass [kg] of ^{234}U to LWB for Partial Mining Scenario

	CRP 1	CRP 2	CRP 3	CRP 4
CRA-2026				
R1	2.92E-02	1.45E-02	3.38E-03	7.62E-03
R2	1.81E-02	2.12E-03	9.62E-10	1.45E-04
R3	2.67E-02	1.89E-02	1.58E-02	9.78E-03
RPPCR				
R1	2.92E-02	1.10E-02	3.38E-03	7.62E-03
R2	1.81E-02	6.67E-04	9.62E-10	1.45E-04
R3	2.67E-02	1.96E-02	1.58E-02	9.78E-03

Table 39. Median Cumulative Mass [kg] of ^{234}U to LWB for Partial Mining Scenario

	CRP 1	CRP 2	CRP 3	CRP 4
CRA-2026				
R1	0.00E+00	0.00E+00	0.00E+00	0.00E+00
R2	0.00E+00	0.00E+00	0.00E+00	0.00E+00
R3	0.00E+00	0.00E+00	0.00E+00	0.00E+00
RPPCR				
R1	0.00E+00	0.00E+00	0.00E+00	0.00E+00
R2	0.00E+00	0.00E+00	0.00E+00	0.00E+00
R3	0.00E+00	0.00E+00	0.00E+00	0.00E+00

Table 40. Maximum Cumulative Mass [kg] of ^{234}U to LWB for Partial Mining Scenario

	CRP 1	CRP 2	CRP 3	CRP 4
CRA-2026				
R1	6.97E-01	5.84E-01	1.88E-01	7.62E-01
R2	1.04E+00	1.20E-01	6.88E-08	1.45E-02
R3	9.97E-01	8.89E-01	9.91E-01	9.78E-01
RPPCR				
R1	6.97E-01	5.51E-01	1.88E-01	7.62E-01
R2	1.04E+00	5.21E-02	6.88E-08	1.45E-02
R3	9.97E-01	9.40E-01	9.91E-01	9.78E-01

Information Only

Table 41. Mean Cumulative Mass [kg] of ^{230}Th to LWB for Full Mining Scenario

	CRP 1	CRP 2	CRP 3	CRP 4
CRA-2026				
R1	3.69E-05	1.22E-06	2.36E-05	5.87E-04
R2	9.67E-05	5.40E-06	4.24E-07	6.53E-04
R3	5.36E-05	3.87E-05	9.32E-06	7.45E-04
RPPCR				
R1	3.69E-05	9.51E-07	2.36E-05	5.87E-04
R2	9.67E-05	2.96E-06	4.24E-07	6.53E-04
R3	5.36E-05	3.23E-05	9.32E-06	7.45E-04

Table 42. Median Cumulative Mass [kg] of ^{230}Th to LWB for Full Mining Scenario

	CRP 1	CRP 2	CRP 3	CRP 4
CRA-2026				
R1	5.09E-13	0.00E+00	1.45E-23	8.90E-07
R2	1.22E-13	0.00E+00	5.08E-24	1.13E-06
R3	5.97E-15	0.00E+00	1.10E-24	1.95E-06
RPPCR				
R1	5.09E-13	0.00E+00	1.45E-23	8.90E-07
R2	1.22E-13	0.00E+00	5.08E-24	1.13E-06
R3	5.97E-15	0.00E+00	1.10E-24	1.95E-06

Table 43. Maximum Cumulative Mass [kg] of ^{230}Th to LWB for Full Mining Scenario

	CRP 1	CRP 2	CRP 3	CRP 4
CRA-2026				
R1	2.39E-03	5.67E-05	1.99E-03	1.39E-02
R2	6.97E-03	3.61E-04	2.03E-05	1.73E-02
R3	2.14E-03	1.45E-03	5.26E-04	2.07E-02
RPPCR				
R1	2.39E-03	5.41E-05	1.99E-03	1.39E-02
R2	6.97E-03	1.67E-04	2.03E-05	1.73E-02
R3	2.14E-03	1.03E-03	5.26E-04	2.07E-02

Information Only

Table 44. Mean Cumulative Mass [kg] of ^{230}Th to LWB for Partial Mining Scenario

	CRP 1	CRP 2	CRP 3	CRP 4
CRA-2026				
R1	1.66E-06	2.49E-07	2.81E-08	1.39E-06
R2	1.16E-05	2.80E-07	2.40E-15	2.08E-09
R3	1.10E-05	1.31E-05	8.42E-06	4.20E-06
RPPCR				
R1	1.66E-06	2.00E-07	2.81E-08	1.39E-06
R2	1.16E-05	1.66E-08	2.40E-15	2.08E-09
R3	1.10E-05	1.32E-05	8.42E-06	4.20E-06

Table 45. Median Cumulative Mass [kg] of ^{230}Th to LWB for Partial Mining Scenario

	CRP 1	CRP 2	CRP 3	CRP 4
CRA-2026				
R1	0.00E+00	0.00E+00	0.00E+00	0.00E+00
R2	0.00E+00	0.00E+00	0.00E+00	0.00E+00
R3	0.00E+00	0.00E+00	0.00E+00	0.00E+00
RPPCR				
R1	0.00E+00	0.00E+00	0.00E+00	0.00E+00
R2	0.00E+00	0.00E+00	0.00E+00	0.00E+00
R3	0.00E+00	0.00E+00	0.00E+00	0.00E+00

Table 46. Maximum Cumulative Mass [kg] of ^{230}Th to LWB for Partial Mining Scenario

	CRP 1	CRP 2	CRP 3	CRP 4
CRA-2026				
R1	1.40E-04	2.27E-05	2.60E-06	1.37E-04
R2	9.63E-04	2.57E-05	1.15E-13	2.08E-07
R3	8.92E-04	7.25E-04	6.10E-04	4.20E-04
RPPCR				
R1	1.40E-04	1.87E-05	2.60E-06	1.37E-04
R2	9.63E-04	7.26E-07	1.15E-13	2.08E-07
R3	8.92E-04	7.81E-04	6.10E-04	4.20E-04

Information Only

Table 47. Cumulative Mass to LWB [Count > 10^{-9} kg] of ^{241}Am for Full Mining Scenario

	CRP 1	CRP 2	CRP 3	CRP 4
CRA-2026				
R1	3	1	3	29
R2	3	0	1	30
R3	1	0	1	22
RPPCR				
R1	3	1	3	29
R2	3	0	1	30
R3	1	0	1	22

Table 48. Cumulative Mass to LWB [Count > 10^{-9} kg] of ^{241}Am for Partial Mining Scenario

	CRP 1	CRP 2	CRP 3	CRP 4
CRA-2026				
R1	0	0	0	1
R2	0	0	0	1
R3	0	0	0	0
RPPCR				
R1	0	0	0	1
R2	0	0	0	1
R3	0	0	0	0

Table 49. Cumulative Mass to LWB [Count > 10^{-9} kg] of ^{239}Pu for Full Mining Scenario

	CRP 1	CRP 2	CRP 3	CRP 4
CRA-2026				
R1	24	7	6	49
R2	14	5	6	55
R3	17	5	12	46
RPPCR				
R1	24	5	6	49
R2	14	5	6	55
R3	17	5	12	46

Information Only

Table 50. Cumulative Mass to LWB [Count > 10^{-9} kg] of ^{239}Pu for Partial Mining Scenario

	CRP 1	CRP 2	CRP 3	CRP 4
CRA-2026				
R1	4	1	0	1
R2	2	2	0	1
R3	4	3	2	3
RPPCR				
R1	4	0	0	1
R2	2	1	0	1
R3	4	3	2	3

Table 51. Cumulative Mass to LWB [Count > 10^{-9} kg] of ^{234}U for Full Mining Scenario

	CRP 1	CRP 2	CRP 3	CRP 4
CRA-2026				
R1	42	15	22	70
R2	41	19	24	66
R3	42	24	17	70
RPPCR				
R1	42	15	22	70
R2	41	16	24	66
R3	42	23	17	70

Table 52. Cumulative Mass to LWB [Count > 10^{-9} kg] of ^{234}U for Partial Mining Scenario

	CRP 1	CRP 2	CRP 3	CRP 4
CRA-2026				
R1	15	12	5	3
R2	16	10	4	3
R3	18	11	5	4
RPPCR				
R1	15	12	5	3
R2	16	10	4	3
R3	18	10	5	4

Information Only

Table 53. Cumulative Mass to LWB [Count > 10^{-9} kg] of ^{23A}Th for Full Mining Scenario

	CRP 1	CRP 2	CRP 3	CRP 4
CRA-2026				
R1	20	5	9	50
R2	16	6	10	52
R3	20	7	6	50
RPPCR				
R1	20	4	9	50
R2	16	3	10	52
R3	20	6	6	50

Table 54. Cumulative Mass to LWB [Count > 10^{-9} kg] of ^{23A}Th for Partial Mining Scenario

	CRP 1	CRP 2	CRP 3	CRP 4
CRA-2026				
R1	5	3	0	1
R2	5	2	0	0
R3	4	4	1	2
RPPCR				
R1	5	3	0	1
R2	5	1	0	0
R3	4	4	1	2

Table 55. Cumulative Mass to LWB [Count > 10^{-9} kg] of ^{230}Th for Full Mining Scenario

	CRP 1	CRP 2	CRP 3	CRP 4
CRA-2026				
R1	38	15	14	71
R2	33	13	17	71
R3	34	20	12	70
RPPCR				
R1	38	15	14	71
R2	33	9	17	71
R3	34	19	12	70

Information Only

Table 56. Cumulative Mass to LWB [Count > 10^{-9} kg] of ^{230}Th for Partial Mining Scenario

	CRP 1	CRP 2	CRP 3	CRP 4
CRA-2026				
R1	15	10	2	2
R2	12	5	0	1
R3	12	6	4	2
RPPCR				
R1	15	8	2	2
R2	12	4	0	1
R3	12	6	4	2

5.4 Sensitivity Analysis

The WIPP sensitivity analysis software STEPWISE was used to perform stepwise ranked regression to determine the input variables most strongly associated with uncertainty in cumulative mass transport results of ^{241}Am, ^{239}Pu, ^{234}U, and ^{23A}Th. Partial mining scenario releases are too small to expect meaningful sensitivities. The only differences in sensitivity between the CRA-2026 and RPPCR occur for CRP 2 results due to the small change in location. Accordingly, only CRP 2 full mining simulation sensitivity results are provided.

Table 57 through Table 64 present cumulative correlation R-squared values and correlation coefficients by radionuclide of the top three ranked regression variables for the CRA-2026 and the RPPCR. The R-square column reports cumulative value with entry of each variable into regression model. The last column reports the standardized Rank Regression Coefficient (SRRC). Independent variables identified by the analysis include matrix distribution coefficient for each radionuclide L (MKD_L; e.g. MKD_PU), DTRKMF travel times (DTRK_TIME), climate index (CLIMTIDX), half-matrix block length (HMBLKLT), advective porosity (APOROS), and are reported at various ranks in the tables for the CRA-2026 and the RPPCR. The RPPCR reported sensitivities for CRP 1 and CRP 4 neither of which identified diffusive porosity (DPOROS). The CRP 2 analysis for CRA-2026 and RPPCR shown here identifies DPOROS as influential on uncertainty in ^{234}U and ^{23A}Th releases, although at low ranks with low R-squared values.

MKD is the input variable with the strongest uncertainty association with releases of each radionuclide, except for ^{241}Am where APOROS has the strongest uncertainty association. However, ^{241}Am reports low R-square values for variable APOROS in the CRA-2026 (0.115) and RPPCR (0.100) indicating weak uncertainty association. In the case of ^{241}Am, extremely low mass transport results may be challenging the ability of STEPWISE to identify impactful variables. For example, the partial mining scenario for ^{241}Am reports only a single instance where cumulative 10,000-yr mass to LWB is > 10^{-9} kg.

Information Only

As in the RPPCR for CRP 1 and CRP 4, MKD_L is the only independent variable from the CRP 2 analysis that exceeds an R-square of 0.20. The MKD correlation is negative, indicating that lower matrix distribution coefficients are associated with larger releases. The negative correlation is expected because lower MKD values indicate lower sorption capacity which can lead to higher mass breakthrough occurring faster. The dual porosity transport parameter APOROS emerges as a secondary control, and also has a negative correlation, indicating that lower advective porosity is associated with larger releases. CRP 2 rank correlations between the CRA-2026 and RPPCR are similar, with exception of ^{234}U replicate 2 where MKD_U has the strongest uncertainty association in the CRA-2026 but is not present in the RPPCR. However, rank correlations between the CRA-2026 and RPPCR are unchanged in replicate 1 and 3.

HMBLKLT shows strongest positive correlations, indicating that larger HMBLKT values are associated with larger releases. The half-block length is used to calculate the fracture aperture in the mass-transfer equation. A higher half-block length results in a higher fracture aperture, lower specific surface area for mass transfer, and thereby lower rate of mass transfer between the advective and diffusive domains.

Because of the potential for cross-correlations with the DTRKMF particle travel times, the mining factor could not be included as an independent variable in the STEPWISE analysis. The RPPCR assessed the effect the mining factor has on the results by rank correlating DTRKMF travel times to the LWB against the mining factor parameter (MINP_FAC). The mining factor showed weak to moderate positive correlation with particle travel times in CRP 2 for partial and full mining scenarios in the in the RPPCR (Bethune 2023). This holds true for the CRA-2026, with CRP 2 showing only slight differences (Figure 20).

Table 57. Stepwise Ranked Regression of ^{241}Am for CRA-2026 CRP 2 Full Mining Scenario

Replicate	Step	Variable	R-Square	SRRC
1	1	APOROS	0.11533	-0.32139
1	2	MKD_AM	0.19059	-0.26772
1	3	CLIMTIDX	0.23787	0.21785
2	1	HMBLKLT	0.11244	0.34142
2	2	CLIMTIDX	0.19078	0.28154
2	3	APOROS	0.24557	-0.23066
3	1	APOROS	0.10022	-0.32833
3	2	HMBLKLT	0.18367	0.28346
3	3	MKD_AM	0.23956	-0.23649

Information Only

Table 58. Stepwise Ranked Regression of ^{241}Am for RPPCR CRP 2 Full Mining Scenario

Replicate	Step	Variable	R-Square	SRCC
1	1	APOROS	0.09999	-0.29969
1	2	MKD_AM	0.15287	-0.22191
1	3	CLIMTIDX	0.199	0.20904
2	1	HMBLKLT	0.09521	0.31316
2	2	APOROS	0.1817	-0.29447
2	3	CLIMTIDX	0.26246	0.2829
3	1	APOROS	0.11625	-0.35604
3	2	HMBLKLT	0.23549	0.34217
3	3	MKD_AM	0.28501	-0.23124

Table 59. Stepwise Ranked Regression of ^{239}Pu for CRA-2026 CRP 2 Full Mining Scenario

Replicate	Step	Variable	R-Square	SRRC
1	1	MKD_PU	0.21897	-0.45904
1	2	APOROS	0.38575	-0.40133
1	3	HMBLKLT	0.43043	0.21153
2	1	MKD_PU	0.19913	-0.47244
2	2	APOROS	0.36645	-0.42517
2	3	CLIMTIDX	0.46992	0.30602
3	1	MKD_PU	0.2432	-0.48584
3	2	APOROS	0.28124	-0.20161
3	3	HMBLKLT	0.31989	0.19687

Information Only

Table 60. Stepwise Ranked Regression of ^{239}Pu for RPPCR CRP 2 Full Mining Scenario

Replicate	Step	Variable	R-Square	SRRC
1	1	MKD_PU	0.29341	-0.53517
1	2	APOROS	0.39649	-0.31407
1	3	HMBLKLT	0.44001	0.20875
2	1	MKD_PU	0.19685	-0.46549
2	2	APOROS	0.37436	-0.43575
2	3	CLIMTIDX	0.45837	0.27352
3	1	MKD_PU	0.25294	-0.50351
3	2	APOROS	0.30636	-0.23834
3	3	HMBLKLT	0.33836	0.18059

Table 61. Stepwise Ranked Regression of ^{234}U for CRA-2026 CRP 2 full mining scenario

Replicate	Step	Variable	R-Square	SRRC
1	1	MKD_U	0.41707	-0.68499
1	2	APOROS	0.55749	-0.38266
1	3	DPOROS	0.58571	-0.16813
2	1	MKD_U	0.45859	-0.7563
2	2	DTRK_TIME	0.56203	-0.33394
2	3	APOROS	0.6701	-0.33006
3	1	MKD_U	0.52297	-0.63711
3	2	DTRK_TIME	0.5908	-0.26018
3	3	APOROS	0.62166	-0.18166

Information Only

Table 62. Stepwise Ranked Regression of ^{234}U for RPPCR CRP 2 Full Mining Scenario

Replicate	Step	Variable	R-Square	SRRC
1	1	MKD_U	0.42106	-0.68609
1	2	APOROS	0.54966	-0.3666
1	3	DPOROS	0.57967	-0.17338
2	1	DTRK_TIME	0.58274	-0.31183
2	2	APOROS	0.65808	-0.27644
2	3	DPOROS	0.67295	-0.12426
3	1	MKD_U	0.47418	-0.6277
3	2	DTRK_TIME	0.50722	-0.1917

Table 63. Stepwise Ranked Regression of ^{23A}Th for CRA-2026 CRP 2 Full Mining Scenario

Replicate	Step	Variable	R-Square	SRRC
1	1	MKD_TH	0.29007	-0.57653
1	2	APOROS	0.35134	-0.2915
1	3	DTRK_TIME	0.43222	-0.2804
2	1	MKD_TH	0.34827	-0.61803
2	2	APOROS	0.43266	-0.30775
2	3	CLIMTIDX	0.50239	0.24769
3	1	MKD_TH	0.37284	-0.58285
3	2	APOROS	0.47201	-0.29483
3	3	DTRK_TIME	0.53089	-0.25164

Information Only

Table 64. Stepwise Ranked Regression of ^{23A}Th for RPPCR CRP 2 Full Mining Scenario

Replicate	Step	Variable	R-Square	RegCoeff
1	1	MKD_TH	0.30112	-0.57755
1	2	DTRK_TIME	0.37195	-0.30034
1	3	APOROS	0.44957	-0.27446
2	1	MKD_TH	0.35929	-0.6155
2	2	DTRK_TIME	0.4108	-0.24779
2	3	APOROS	0.4691	-0.2423
3	1	MKD_TH	0.32505	-0.55086
3	2	APOROS	0.42888	-0.30008
3	3	DTRK_TIME	0.47821	-0.2328

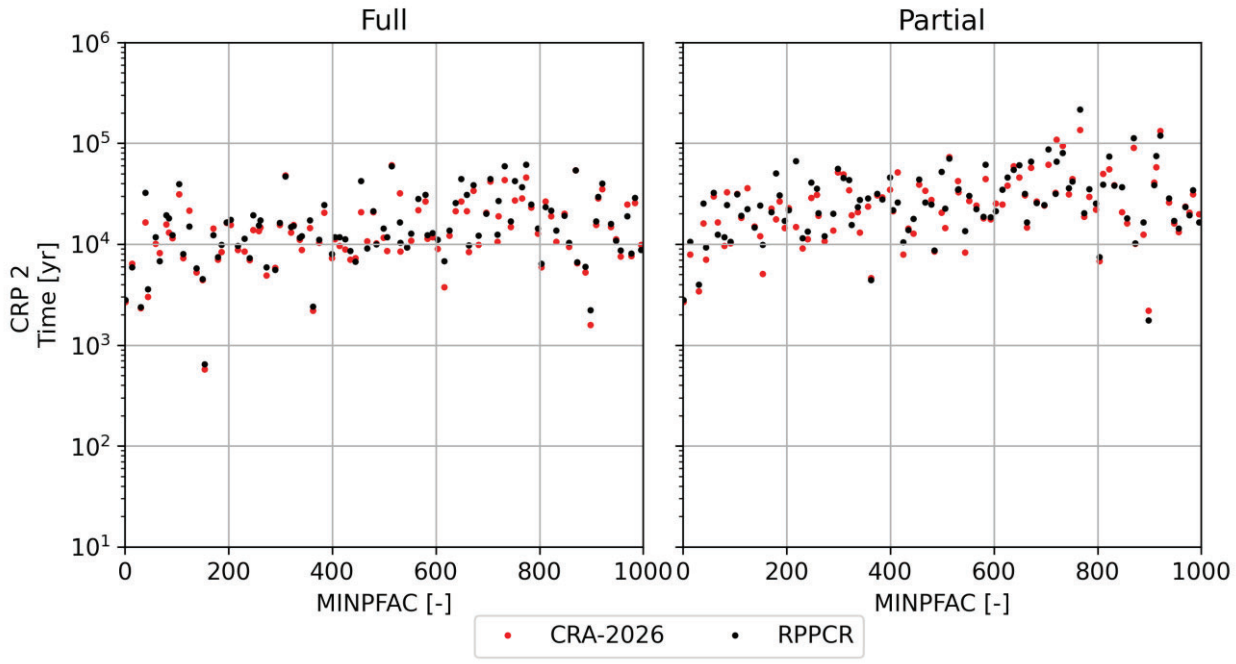

Figure 20. DTRKMF particle travel time to LWB versus mining factor

Information Only

6.0 SUMMARY

The CRA-2026 Culebra flow and transport calculations are presented for four radionuclides ^{241}Am, ^{239}Pu, ^{23A}Th, ^{234}U, and the decay product of ^{234}U, ^{230}Th, for two mining scenarios and four mass release points. Results are reported for all four mass release points, which functionally encompasses Culebra flow and transport results for the CRA-2026 interim and final state repositories. The CRA-2026 PA calculations used the same set of T-field calibrations and Culebra flow and transport parameters as the RPPCR PA (King and Zeitler 2025). Results are compared to the RPPCR. The only change impacting results was a small change in location of CRP 2.

Culebra flow fields in CRA-2026 are unchanged relative to the RPPCR resulting in identical flow rates that show a linear north-south high-transmissivity feature located in the southern half of the domain, and irregular shaped regions originating from the edges of potash mining scenarios.

As reported in the RPPCR particles released in the full mining scenario at CRP 4 travel relatively quickly to the western edge of the WIPP LWB and exit the LWB significantly earlier than the other scenarios across all probability levels. Particle travel times from CRP 2 in the CRA-2026 and RPPCR exhibit a strong correlation for both the full and partial mining scenarios, with correlation values of 0.97 and 0.88 respectively. Particle tracks from CRP 2 show slight differences between CRA-2026 and RPPCR, and travel times to the LWB are slightly shorter in the CRA-2026 relative to the RPPCR at most probabilities.

Mass transport results are nearly identical between the CRA-2026 and RPPCR. Full mining scenario mass transport results show earlier, more complete, and more frequent breakthrough than the partial mining scenario for all radionuclides and release points, particularly for CRP 4. In the full mining scenario, CRP 2 and CRP 3 releases are generally lower than CRP 1, which in turn are lower than CRP 4, for all radionuclides. Cumulative mass transported to the LWB from ^{241}Am are typically lowest and ^{234}U are the highest, with the ^{23A}Th and ^{239}Pu values in-between, for all release points and mining scenarios. ^{234}U has near complete breakthrough from all release points in the full mining scenario, and the largest cumulative mass breakthrough in the partial mining scenario. Mass transport results from the CRA-2026 CRP 2 are biased toward slight increases in cumulative mass breakthrough relative to the RPPCR.

The independent variable most strongly associated with uncertainty in mass discharge for CRP 2 simulations is the matrix distribution coefficient (MKD_L). The dual porosity transport parameter (APOROS) emerges as a secondary control. The mining factor showed weak to moderate positive correlation with DTKRMF particle travel times in CRP 2 for partial and full mining scenarios.

Information Only

7.0 REFERENCES

Bakker, M., Post, V., Langevin, C. D., Hughes, J. D., White, J. T., Starn, J. J., & Fienen, M. N. (2016). Scripting MODFLOW model development using Python and FloPy. *Groundwater*, *54*(5), 733-739.

Bethune, J. and S. Brunell. 2022. Determination of Culebra Release Points Number and Locations in a Repository with New Panels. ERMS 576493. Carlsbad, NM: Sandia National Laboratories.

Bethune, J. 2023. Culebra Flow and Transport Analysis Report for the Replacement Panels Planned Change Request (RPPCR). ERMS 579725. Carlsbad, NM: Sandia National Laboratories.

Bollinger, M. 2024. Letter to Ms. L. Veal. Subject: Planned Change Request for the use of Replacement Panels 11 and 12. March 12, 2024. CBFO:ERCD:MG:SV:24-0168. Carlsbad, NM: U.S. DOE, Carlsbad Field Office.

Bowman, D., R. Kushnereit, M. Pedrazas, P. Johnson, N. Deeds, and J. Pinkard. 2023. Analysis Report Documenting the Data, Generation, and Calibration of T-fields for CRA-2024. ERMS 579507. Carlsbad, NM: Sandia National Laboratories.

Burgess, A., T. Doe, T. Lowenstein, and J.A. Thies. 2008. Waste Isolation Pilot Plant Culebra Hydrogeologic Conceptual Model Peer Review Final Report. Carlsbad, NM: U.S. Department of Energy. ERMS 551513.

Corbet, T. 1995. Record of FEP Screening Work FEP 10# NS-9 Justification of SEC02D Approximation for PA Transport Calculation. ERMS 230802. Carlsbad, NM: Sandia National Laboratories.

Corbet, T. and P. Swift. 1996. Parameters required for SECOFL2D: Climate Index. ERMS 237465. Carlsbad, NM: Sandia National Laboratories.

Cranston, C.C. 2009. Minable Potash Ore. ERMS 551120. Carlsbad, NM: Bureau of Land Management.

Hansen, C., S. Brunell, B. Day, S. King, and J. Wilgus. 2025. Analysis Plan for the 2026 WIPP Compliance Recertification Application Performance Assessment. AP-214. Carlsbad, NM: Sandia National Laboratories.

Hansen, C.W. 2021. Review of Conceptual Models for the Additional Panels Performance Assessment. ERMS 575523. Carlsbad, NM. Sandia National Laboratories.

Hart, D.B., R.M. Holt, and S.A. McKenna. 2008. Analysis Report for Task 5 of AP-114: Generation of Revised Base Transmissivity Fields. ERMS 552391. Carlsbad, NM: Sandia National laboratories.

Holt, R.M. 1997. Conceptual Model for Transport Processes in the Culebra Dolomite Member of the Rustler Formation. Carlsbad, NM: Sandia National laboratories. SAND 97-0194.\

Kaplan, U., Swanson, J., and Kutahyali-Aslani, C. 2025. LANL ACRSP Parameter Recommendations for CRA-2026 Performance Assessment. Revision 1. LCO-ACP-41. Carlsbad, NM: Los Alamos National Laboratory.

Information Only

King, S., Brunell, S. and Zeitler, T., 2025. Analysis Report for Normalized Releases in the 2026 Compliance Recertification Application Performance Assessment: Interim State Repository. Carlsbad, NM: Sandia National Laboratories.

King, S., and Zeitler, T., 2025. Analysis Report for Parameter Sampling in the 2026 Compliance Recertification Application Performance Assessment. EIMS-0004951492. Carlsbad, NM: Sandia National Laboratories.

Kuhlman, K. 2010. Analysis Report for the CRA-2009 PABC Culebra Flow and Transport Calculations. ERMS 552951. Sandia National Laboratories, Carlsbad, NM.

Kushnereit, R., A. Wahi, and T. Yan. 2020. Culebra Release Point Reassessment Analysis Report. ERMS 574216. Carlsbad, NM: Sandia National Laboratories.

Langevin, C.D., J.D. Hughes, E.R. Banta, R.G. Niswonger, S. Panday, and A.M. Provost. 2017. Documentation for the MODFLOW 6 Groundwater Flow Model. U.S. Geological Survey Techniques and Methods, Book 6, A55. https://doi.org/10.3133/tm6A55.

Long, J. 2023. Computational Code Execution and File Management for the Replacement Panels Planned Change Request (RPPCR). ERMS 579728. Sandia National Laboratories. Carlsbad, NM.

Long, J. 2024. Nuclear Waste Management Procedure NP 19-1 SOFTWARE REQUIREMENTS, Revision 20. Carlsbad, NM: Sandia National Laboratories.

Long, J. 2025. Computational Code Execution and File Management for the 2026 Compliance Recertification Application Performance Assessment (CRA-2026 FS). EIMS-0004899943. Carlsbad, NM: Sandia National Laboratories.

Long, J., and King. S., 2022. Summary Report on the Migration of the WIPP PA Codes from Solaris to Linux. ERMS 577606. Carlsbad, NM: Sandia National Laboratories.

Lowry, T.S. and Kanney, J.F., 2005. Analysis Report for the CRA-2004 PABC Culebra Flow and Transport Calculations. ERMS 541508. Carlsbad, NM: Sandia National Laboratories.

McCormick, J., Kirkes R., and Hansen C. 2024. Conceptual Models in WIPP Performance Assessment. EIMS-0004385596. Carlsbad, NM: Sandia National Laboratories.

Meigs, L.C., Beauheim, R.L. and Jones, T.L., eds., 2000. Interpretation of Tracer Tests Performed in the Culebra Dolomite at the Waste Isolation Pilot Plant Site. SAND 97-3109. Carlsbad, NM: Sandia National Laboratories.

Sjomeling, D. 2019. "2:30 Meeting Information," an email to Paul Shoemaker with the attachment "West Mains and Panels peer review info Final 091219.pdf." ERMS 572682. Carlsbad, NM: Nuclear Waste Partnership LLC. October 17, 2019.

U.S. Environmental Protection Agency (U.S. EPA). 1998. 40 CFR 194: Criteria for the Certification and Recertification of the Waste Isolation Pilot Plant's Compliance with the Disposal Regulations: Certification Decision. Federal Register, vol. 63 (May 18, 1998): 27354-27406.

Information Only

U.S. Environmental Protection Agency (U.S. EPA). 2025. Letter from Abigale Tardif to Mark Bollinger, Subject: EPA's Review and Approval of DOE's RPPCR for Waste Panels 11 and 12 at WIPP. July 31, 2025. Washington, DC: U.S. EPA.

Wilgus, J. and S. Brunell. 2025. Re-Calculation of the Location of Culebra Release Point 2 for Use in WIPP PA Rev. 1. EIMS-0004818700. Carlsbad, NM: Sandia National Laboratories.

WIPP Performance Assessment. 2020. Design Document and User's Manual for DTRKMF, Version 1.02. ERMS 574327. Carlsbad, NM: Sandia National Laboratories.

WIPP Performance Assessment. 2021. User's Manual for LHS, Version 3.00. ERMS 574194. Carlsbad, NM: Sandia National Laboratories.

WIPP Performance Assessment. 2022. Design Document and User's Manual for SECOTP2D Version 1.44. ERMS 573879. Carlsbad, NM: Sandia National Laboratories.

WIPP Performance Assessment. 2023. Software Problem Report SPR 23-001 DTRKMF Version 1.02. ERMS 579912. Carlsbad, NM: Sandia National Laboratories.

WIPP Performance Assessment. 2024a. Software Problem Closure Report SPR 23-001 DTRKMF Version 1.02 . EIMS-0004387188. Carlsbad, NM: Sandia National Laboratories.

WIPP Performance Assessment. 2024b. Design Document and User's Manual for DTRKMF Version 2.00. ERMS 582254. Carlsbad, NM: Sandia National Laboratories.

Information Only

8.0 APPENDIX A – NO-MINING RESULTS

Flow field and particle tracking results from simulations without mining (no mining) are not directly considered in PA calculations but serve as input to the mining modified (full and partial mining) flow fields considered in WIPP PA (see section 4.0 step 3). For the RPPCR, Bowman et al. (2023) updated calibrations of the base T-fields generated by Hart et al. (2008). The CRA-2026 uses the same set of calibrated T-fields as the RPPCR. The updated calibrations warrant reporting and characterization of the no mining flow fields and particle tracks.

8.1 Flow

Figure 21 shows the ensemble average of $\log_{10}$ flow rates for no mining within the LWB for the CRA-2026. CRA-2026 used the same set of T-field as the RPPCR and there were no changes to Culebra flow fields so RPPCR flow rates would be identical to the CRA-2026 results shown here. No-mining flow rates show less variation relative to the full and partial mining flow rates discussed in section 5.1 due to the lack of mining impacted areas. The high-transmissivity pathway described in section 5.1 is still present as a linear north-south feature located in the southern half of the domain.

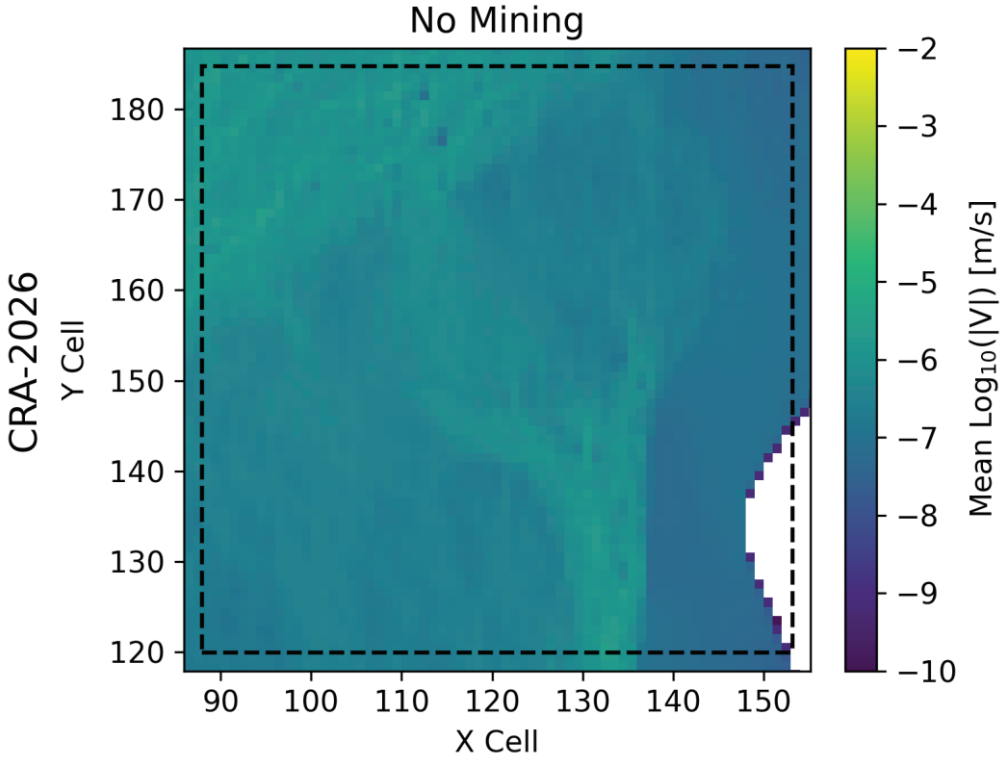

Figure 21. Ensemble Mean Flow Rate for the No-Mining Scenario

Information Only

8.2 Particle Tracking

Figure 22 shows the spatial distribution of all 100 particle tracks alongside the cumulative distribution of the time taken for a particle to reach the LWB from each release point. No-mining particle tracks are similar in character to the partial mining particle tracks which are less influenced by mining affected regions than the full mining results. All four release points show downstream flow generally oriented toward the south. In CRP 1 pathways generally flow toward the high transmissivity feature (described in sections 5.1 and 8.1) and then follow it out of the southern edge of the LWB. This general character can be seen in the particle paths from CRP 2, 3, and 4, but becomes less prominent with western migration of each CRP location away from the high transmissivity feature. Partial mining pathways also show this character, but to a lesser extent due to more broad distribution of particle paths in the east-west direction.

Particles also exit the LWB in the no mining scenario at times similar to partial mining scenario for all four release points. However, no mining results show less variation in particle travel times (Table 65), which could be a function of decreased variation in no mining flow rates. Furthermore, mean and median particle travel times tend to increase with each ascending CRP (Table 65), presumably a consequence of the westward migration of each CRP away from the high transmissivity feature.

Information Only

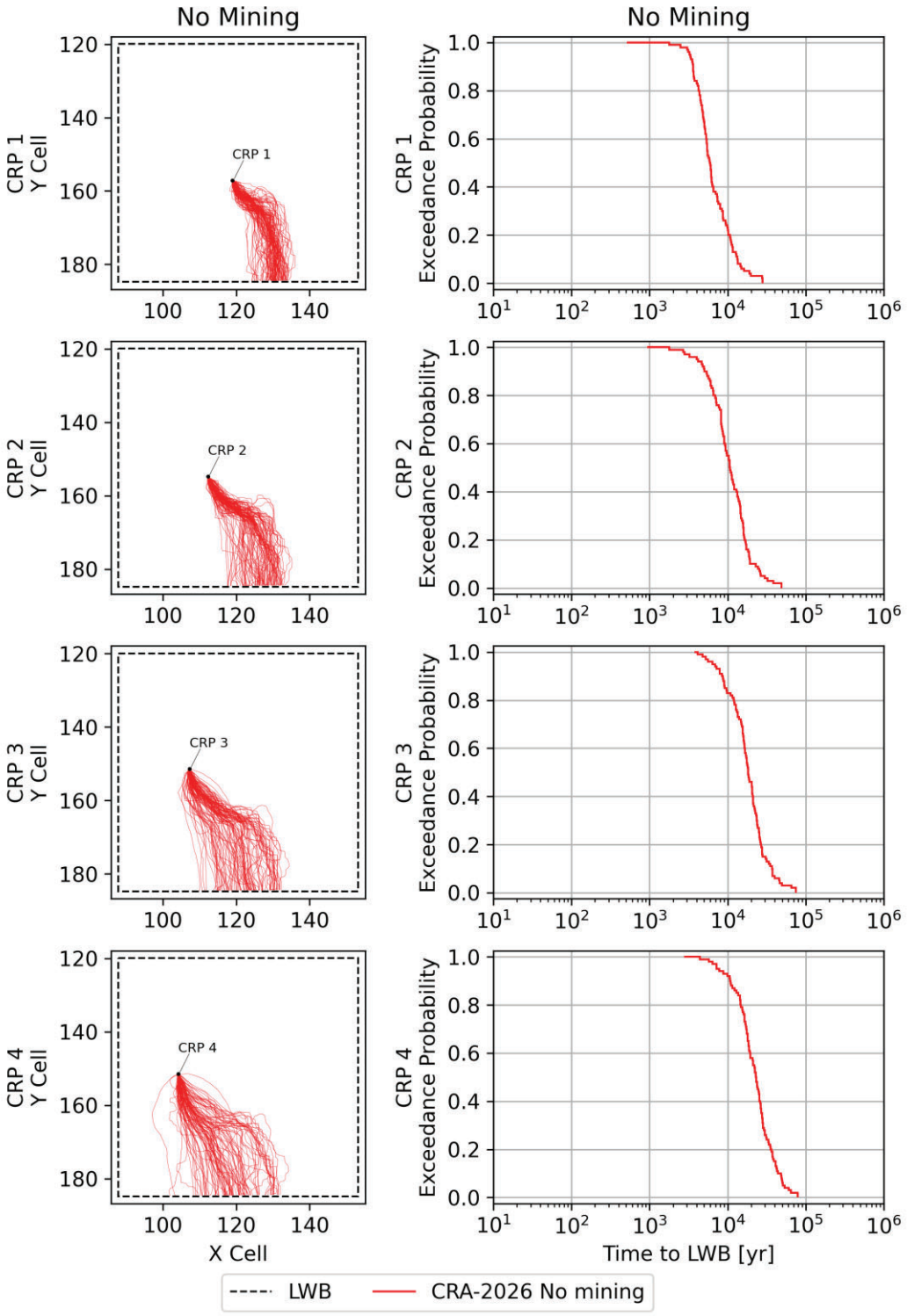

Figure 22. DTRKMF Particle Tracks and Travel Time to LWB Exceedance Probabilities

Information Only

Table 65. Particle Travel Time [yr] to LWB Statistics for the No-Mining Scenario

	CRP 1	CRP 2	CRP 3	CRP 4
Mean	7.38E+03	1.24E+04	2.05E+04	2.51E+04
Median	5.87E+03	1.06E+04	1.83E+04	2.30E+04
Minimum	5.08E+02	9.31E+02	3.74E+03	2.78E+03
Maximum	2.80E+04	4.88E+04	7.45E+04	7.90E+04

8.3 References

Hart, D.B., R.M. Holt, and S.A. McKenna. 2008. Analysis Report for Task 5 of AP-114: Generation of Revised Base Transmissivity Fields. ERMS 549597. Carlsbad, NM: Sandia National Laboratories.

Bowman, D., R. Kushnereit, M. Pedrazas, P. Johnson, N. Deeds, and J. Pinkard. 2023. Analysis Report Documenting the Data, Generation, and Calibration of T-fields for CRA-2024. ERMS 579507. Carlsbad, NM: Sandia National Laboratories.

Information Only